Appendix A.1:

Shirley Intermediate School – VsVp 57203

Table 1: Site Description for Shirley Intermediate School (v_sv_p 57203).

Attribute	Yes/No			Description/Date	Symbol in Figure 1
	10-m Buffer	20-m Buffer	50-m Buffer		
Near a body of surface water or other free face features?	No	No	No	The center of the site is 55 meters away from the unnamed creek. The direction of the free face is roughly NE-SW (the creek runs SW-NE), while its height is approximately 2.5 m.	Blue Outline
Lateral spreading observed during the CES?	No	No	No	Ground cracks indicating lateral spreading were not observed by the mapping team.[1]	NA
Nearby buildings or structures?	No	No	Yes	Several school buildings are approximately 20 m away from the center of the site, localized in the SW portion of the 50-m buffer, and covering 10% of the area.	White Fill + Brown Outline
Sloping land?	No	No	No	Flat land, sports ground.	NA
Step changes in the ground surface?	No	No	No	NA	NA
Retaining walls?	No	No	No	NA	NA
Vegetation?	No	Yes	Yes	Trees cover 10% of the 20-m buffer and 20% of the 50-m buffer. They are located between the E and SE portions of the 20-m buffer and between the NE and SW portions of the 50-m buffer.	White Fill + Green Outline
Anthropogenic changes to the site between the LiDAR surveys?	No	Yes	Yes	Three school buildings were added between Apr 2011 and June 2011 earthquake. They are in the SW quadrant of the 50-m buffer and cover 7% of the area. They also spread to the southern part of the 20-m buffer, affecting 1% of the area. Minor earthwork in the southern portion of the 50-m buffer was performed sometime between Oct 2009 and Feb 2011. It is not visible in Figure 1 because it is in the place of buildings.	White Fill + Brown Outline
Other important factors?	No	Yes	Yes	The soccer goal is located in the SW quadrant of the 20-m buffer. Busy two-way road occupies 15% of the 50-m buffer and stretches throughout the NE and SE quadrants.	Soccer Goal: White Fill + Red Outline Road: White Fill + Gray Outline

Note: Buffer is the area within a circle of a specified radius (10, 20, or 50 m) with VsVp investigations done at its center (172.661995°, -43.510408°).

[1] Canterbury Geotechnical Database. (2012). "Observed Ground Crack Locations", Map Layer CGD0400 - 23 July 2012, retrieved July 09, 2018 from https://canterburygeotechnicaldatabase.projectorbit.com/

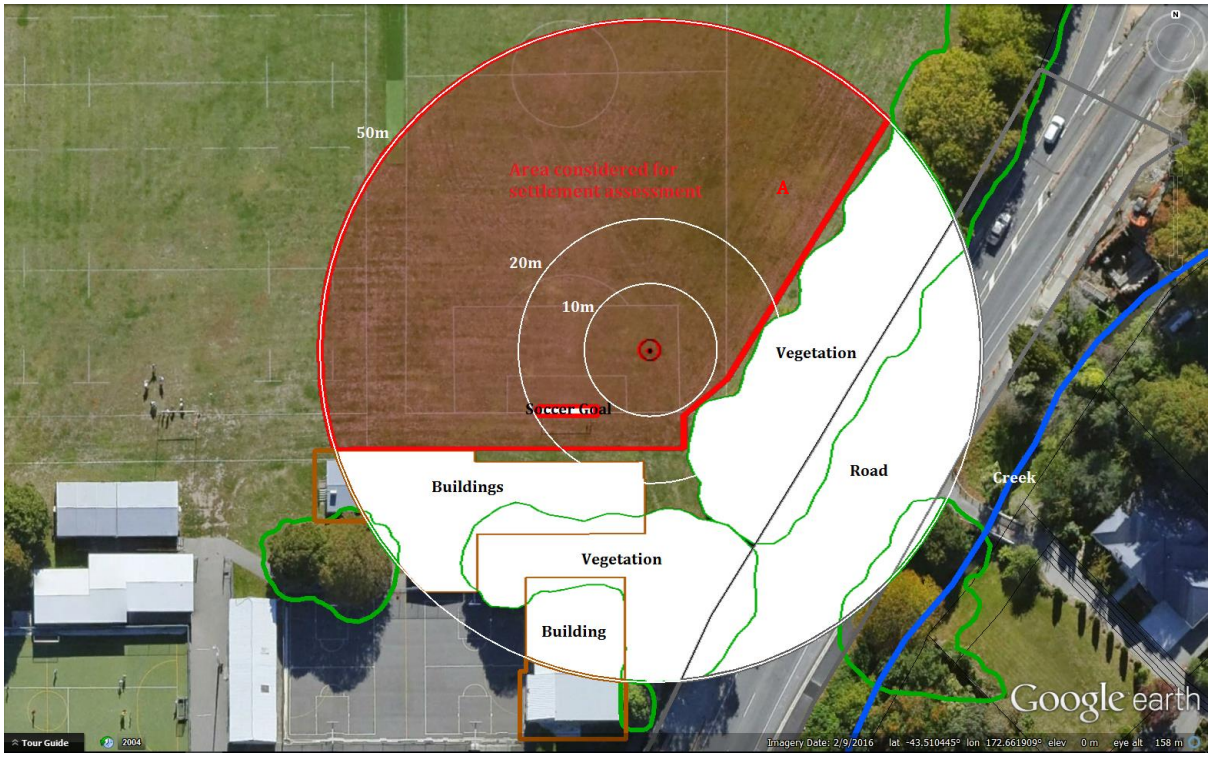

Figure 1: Site plan with areas where LiDAR survey data is considered.

Note 1: The area selected for settlement assessment (Patch A) is free of vegetation, structures, anthropogenic changes, and other important factors that have the potential to influence LiDAR measurements.

Table 2: LiDAR flight error adjustments, global adjustments for the difference between average LiDAR point elevations and benchmark survey elevations, and vertical tectonic movement adjustments.

	Adjustments (mm)		
Earthquake Event(s)	LiDAR Flight Error	Global Offset[2]	Tectonic Vertical Movement
Sep-10	-100	-3	0
Feb-11	100	16	-85
Jun-11	0	38	-40
Dec-11	0	-65	0
CES	0	-14	-125
Any LiDAR survey affected by ejecta?			No

Note: The negative sign indicates the subtraction from the ground surface subsidence, while the positive sign indicates the addition to the ground surface subsidence.

[2] Russell, J., & van Ballegooy, S. (2015). *Canterbury Earthquake Sequence: Increased liquefaction vulnerability assessment methodology*. New Zealand: Tonkin & Taylor Ltd.

Table 3: LiDAR Measurement Error.

Surveys	Buffer	Area Averaged Difference Indicating Repeat Measurement Error (mm)	$\sigma^*_{\text{individual LiDAR points}}$ (mm)	%Reduction in σ due to Area Averaging of LiDAR Points
Post Feb 2011: Mar 2011 and May 2011	10-m	20	59	[20,34]
	20-m	12		
	50-m	18		
Post Dec 2011: Feb 2012 and Oct 2015	10-m	37	70	[53,57]
	20-m	40		
	50-m	69		

*Standard deviation.

Table 4: Ground surface subsidence adjustments due to LiDAR measurement error.

Earthquake Event(s)	$\sigma_{\text{pre-EQ LiDAR survey}}$ (mm)	$\sigma_{\text{post-EQ LiDAR survey}}$ (mm)	σ_{total} (mm)	Area Average Adjusted σ (mm) **
Sep-10	158	56	134	±77
Feb-11	56	59	59	±34
Jun-11	59	61	62	±36
Dec-11	61	70	87	±49
CES	158	70	124	±71

**Based on the highest %Reduction in Table 3.

Table 5: Raw liquefaction-related ground surface subsidence using original LiDAR points.

	Average Ground Surface Subsidence (mm)		
Earthquake Event(s)	10-m Buffer	20-m Buffer	50-m Buffer
Sep-10	134	138	124
Feb-11	214	213	148
Jun-11	114	98	75
Dec-11	7	12	15
CES	469	461	362

Table 6: Corrected liquefaction-related ground surface subsidence using original LiDAR points with the calculated adjustments in Table 2.

	Average Calculated Ground Surface Subsidence (mm)		
Earthquake Event(s)	10-m Buffer	20-m Buffer	50-m Buffer
Sep-10	31±75	35±75	21±75
Feb-11	245±25	244±25	179±25
Jun-11	112±25	96±25	73±25
Dec-11	-58±50	-53±50	-50±50
CES	330±75	322±75	223±75

Notes: Plus/minus values are same as those in Table 4, but rounded to the nearest 25; Positive overall values indicate ground surface subsidence, while negative overall values indicate ground surface uplift.

Table 7: Corrected liquefaction-related ground surface subsidence using LiDAR DEMs.

	Estimated Ground Surface Subsidence (mm)								
	10-m Buffer			20-m Buffer			50-m Buffer		
Earthquake Event(s)	16th %ile	50th %ile	84th %ile	16th %ile	50th %ile	84th %ile	16th %ile	50th %ile	84th %ile
Sep-10	<50	50	50	<50	50	50	<50	50	50
Feb-11	200	200	250	200	250	250	150	150	250
Jun-11	150	150	150	50	50	150	50	50	150
Dec-11	50	50	50	50	50	50	50	50	50
CES	450	450	450	350	350	450	250	350	450

Note: These percentiles are not the exact statistical measures; they indicate the spatial variability of ground surface subsidence.

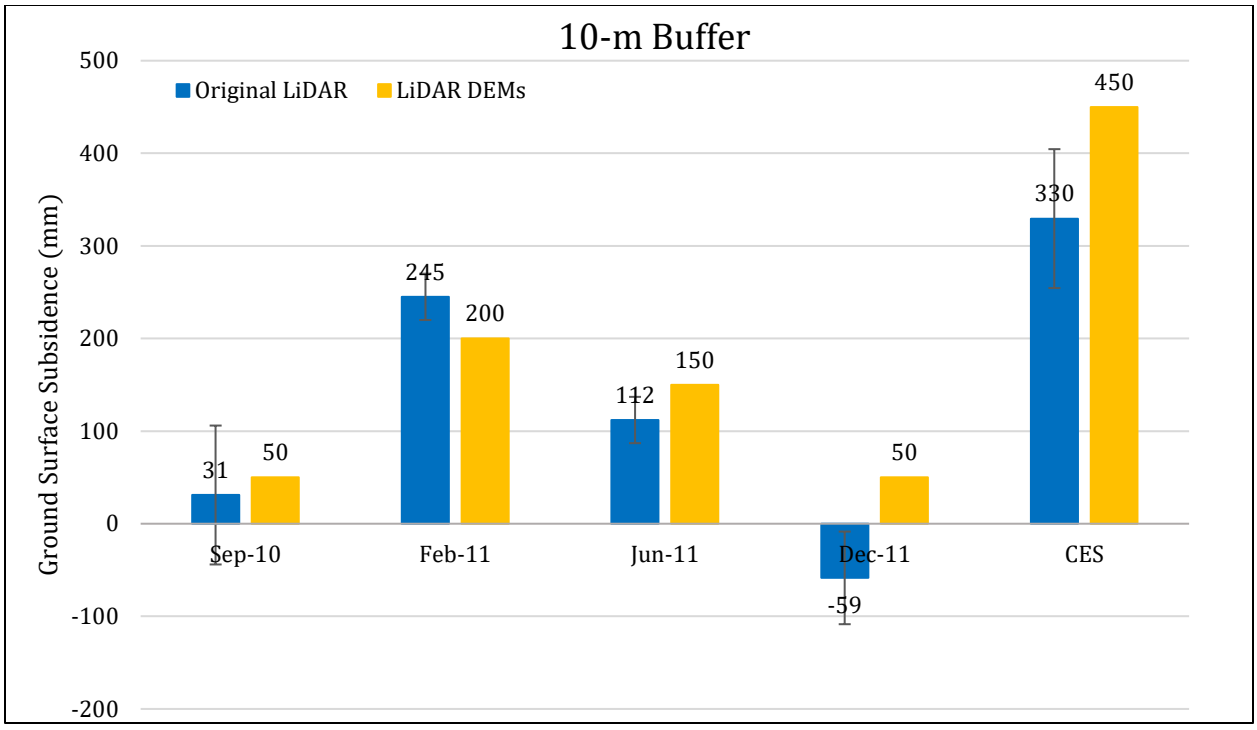

Figure 2: Comparison between ground surface subsidence determined from original LiDAR survey points and ground surface subsidence (50th %ile) estimated using LiDAR DEMs for the 10-m buffer.

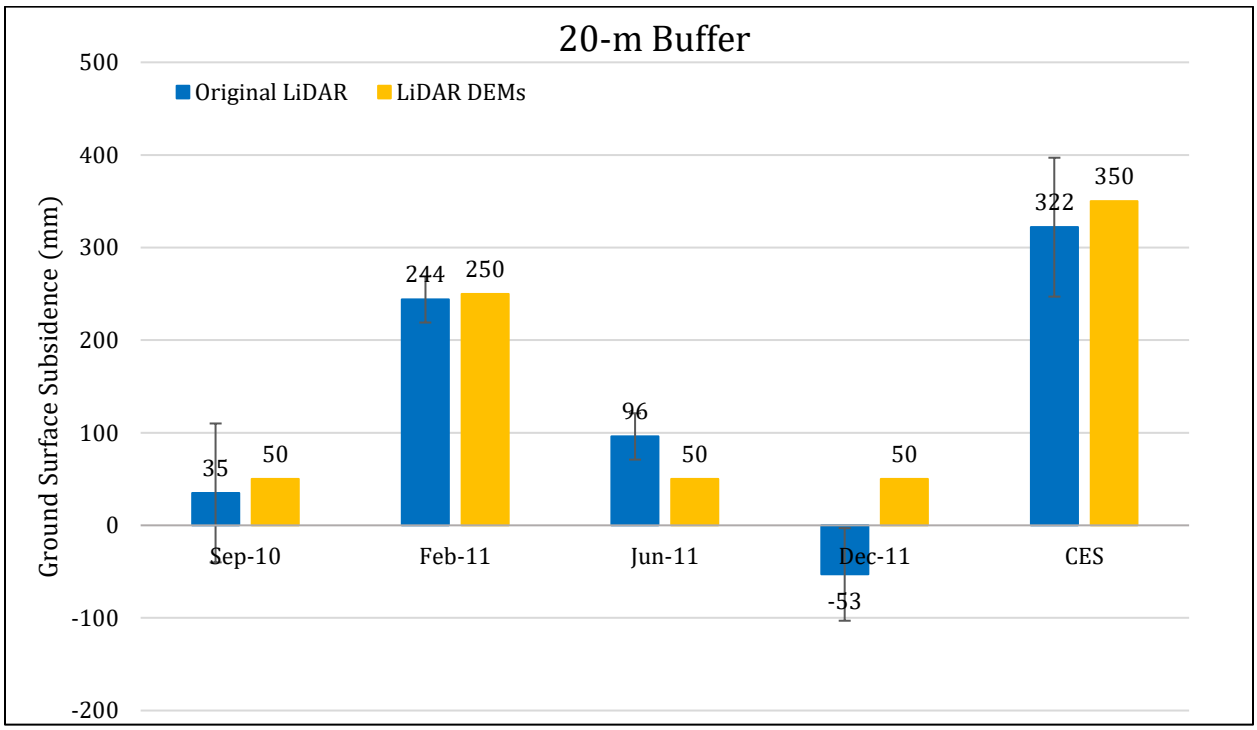

Figure 3: Comparison between ground surface subsidence determined from original LiDAR survey points and ground surface subsidence (50th %ile) estimated using LiDAR DEMs for the 20-m buffer.

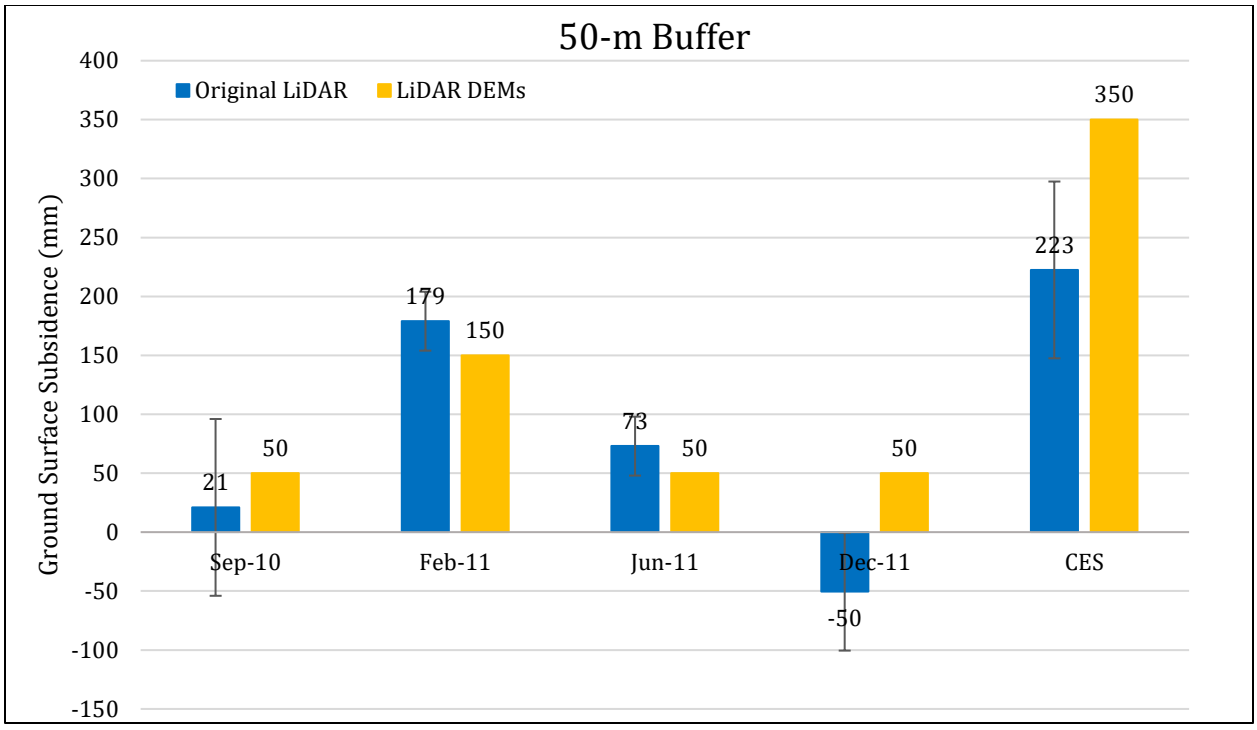

Figure 4: Comparison between ground surface subsidence determined from original LiDAR survey points and ground surface subsidence (50th %ile) estimated using LiDAR DEMs for the 50-m buffer.

Note 2: The ground surface subsidence values determined from original LiDAR survey points are similar to the ground surface subsidence values estimated using LiDAR DEMs for all earthquake events.

Table 8a: Ejecta-Induced settlement for the top 20 m of the soil profile within the 10-m buffer for the 50th %ile PGA, P_L=50%, and C_{FC}=0.13 using BI-2014, ZRB-2002, and I_C cutoff of 2.6.

Earthquake Event	M_W	PGA (g)	Depth to Groundwater (m)	S_T (mm)	S_{V1D} (mm)	$S_{E,L}$ (mm)
Sep-10	7.1	0.19	2.5	31±75	7±20	24±78
Feb-11	6.2	0.38	2.5	245±25	71±50	174±56
Jun-11	6.2	0.22	2.2	112±25	10±25	102±35
Dec-11	6.1	0.26	2.0	-58±50	25±50	-83±71

Notes: S_T = Total settlement (Table 6); S_{V1D} = Average vertical settlement due to volumetric compression using Boulanger and Idriss (2014) (BI-2014) and Zhang et al. (2002) (ZRB-2002) procedures and de Greef and Lengkeek (2018) thin-layer correction; $S_{E,L}$ = Ejecta-induced settlement as the difference between the LiDAR-based S_T and S_{V1D}.

Table 8b: Ejecta-Induced settlement for the top 20 m of the soil profile within the 20-m buffer for the 50th %ile PGA, P_L=50%, and C_{FC}=0.13 using BI-2014, ZRB-2002, and I_C cutoff of 2.6.

Earthquake Event	M_W	PGA (g)	Depth to Groundwater (m)	S_T (mm)	S_{V1D} (mm)	$S_{E,L}$ (mm)
Sep-10	7.1	0.19	2.5	35±75	7±20	28±78
Feb-11	6.2	0.38	2.5	244±25	71±50	173±56
Jun-11	6.2	0.22	2.2	96±25	10±25	86±35
Dec-11	6.1	0.26	2.0	-53±50	25±50	-78±71

Notes: S_T = Total settlement (Table 6); S_{V1D} = Average vertical settlement due to volumetric compression using Boulanger and Idriss (2014) (BI-2014) and Zhang et al. (2002) (ZRB-2002) procedures and de Greef and Lengkeek (2018) thin-layer correction; $S_{E,L}$ = Ejecta-induced settlement as the difference between the LiDAR-based S_T and S_{V1D}.

Table 8c: Ejecta-Induced settlement for the top 20 m of the soil profile for within the 50-m buffer for the 50th %ile PGA, P_L=50%, and C_{FC}=0.13 using BI-2014, ZRB-2002, and I_C cutoff of 2.6.

Earthquake Event	M_W	PGA (g)	Depth to Groundwater (m)	S_T (mm)	S_{V1D} (mm)	$S_{E,L}$ (mm)
Sep-10	7.1	0.19	2.5	21±75	3±20	18±78
Feb-11	6.2	0.38	2.5	179±25	38±50	141±56
Jun-11	6.2	0.22	2.2	73±25	5±25	68±35
Dec-11	6.1	0.26	2.0	-50±50	13±50	-63±71

Notes: S_T = Total settlement (Table 6); S_{V1D} = Average vertical settlement due to volumetric compression using Boulanger and Idriss (2014) (BI-2014), Zhang et al. (2002) (ZRB-2002) procedures and de Greef and Lengkeek (2018) thin-layer correction; $S_{E,L}$ = Ejecta-induced settlement as the difference between the LiDAR-based S_T and S_{V1D}.

Note 3: The uncertainty for volumetric settlement was derived based on the sensitivity of volumetric settlement to PGA, C_{FC}, and P_L for each earthquake event for VsVp 57203 *Shirley Intermediate School* and CC LIQ 1 – CPT 5586 – *Vivian St* sites. Taking the 50th percentile as the baseline case, the minimum and maximum values corresponding to the difference between the 25th percentile and the 50th percentile and the 75th percentile and the 50th percentile were determined. The arithmetic mean of the range of the minimum and maximum difference was evaluated for each patch at the two sites. The maximum arithmetic mean for each earthquake event was rounded to the nearest five and used as the uncertainty value. Accordingly, the 1-D volumetric settlement uncertainties of ±20, ±50, ±25, and ±50 mm for the Sep-10, Feb-11, Jun-11, and Dec-11 earthquake events, respectively, were used for all sites in this study.

Table 9a: Coverage area and height of ejecta estimates for the 10-m buffer using photographs.

Earthquake Event	$A_{E,thick}$ (m^2)	$H_{E,thick}$ (mm)	$A_{E,thin}$ (m^2)	$H_{E,thin}$ (mm)	A_T (m^2)
Sep-10	0	0	0	0	314
Feb-11	143	150-250	39	50-100	314
Jun-11	94*	30-100*	0	0	269**
Dec-11	0	0	3	10-20	314

Notes: $A_{E,thick/thin}$ = Coverage area of thick/thin ejecta layers; $H_{E,thick/thin}$ = Lower-upper estimate of height of thick/thin ejecta layers; A_T = Total assessment area of a buffer being considered; Thin and thick layers correspond to light gray and dark gray colors of ejecta observed in aerial photographs; * denotes the area and height of ejecta layers with an intermediate thickness due to the uncertainty associated with cleaning of ejecta; ** indicates that A_T is lower due to the presence of objects (e.g., vehicles and construction equipment/material) at portions of the site at the time the aerial photograph was acquired.

Table 9b: Coverage area and height of ejecta estimates for the 20-m buffer using photographs.

Earthquake Event	$A_{E,thick}$ (m^2)	$H_{E,thick}$ (mm)	$A_{E,thin}$ (m^2)	$H_{E,thin}$ (mm)	A_T (m^2)
Sep-10	0	0	0	0	1003
Feb-11	594	150-250	171	50-100	1003
Jun-11	439*	30-100*	0	0	938**
Dec-11	0	0	18	10-20	1003

Notes: $A_{E,thick/thin}$ = Coverage area of thick/thin ejecta layers; $H_{E,thick/thin}$ = Lower-upper estimate of height of thick/thin ejecta layers; A_T = Total assessment area of a buffer being considered; Thin and thick layers correspond to light gray and dark gray colors of ejecta observed in aerial photographs; * denotes the area and height of ejecta layers with an intermediate thickness due to the uncertainty associated with cleaning of ejecta; ** indicates that A_T is lower due to the presence of objects (e.g., vehicles and construction equipment/material) at portions of the site at the time the aerial photograph was acquired.

Table 9c: Coverage area and height of ejecta estimates for the 50-m buffer using photographs.

Earthquake Event	$A_{E,thick}$ (m^2)	$H_{E,thick}$ (m)	$A_{E,thin}$ (m^2)	$H_{E,thin}$ (m)	A_T (m^2)
Sep-10	0	0	0	0	4061
Feb-11	1413	150-250	322	50-100	4061
Jun-11	1191*	30-100*	0	0	3944**
Dec-11	0	0	55	10-20	4061

Notes: $A_{E,thick/thin}$ =Coverage area of thick/thin ejecta layers; $H_{E,thick/thin}$ = Lower-upper estimate of height of thick/thin ejecta layers; A_T= Total assessment area of a buffer being considered; Thin and thick layers correspond to light gray and dark gray colors of ejecta observed in aerial photographs; * denotes the area and height of ejecta layers with an intermediate thickness due to the uncertainty associated with cleaning of ejecta; ** indicates that A_T is lower due to the presence of objects (e.g., vehicles and construction equipment/material) at portions of the site at the time the aerial photograph was acquired.

Note 4: The values in Table 9 correspond to the coverage area of ejecta outlined in aerial photographs (Figures 60 through 63) and the lower and upper estimates of ejecta height based on residents' reports (e.g., https://www.odt.co.nz/lifestyle/magazine/all-one-one-all) and ground photographs taken in neighboring areas. The ejecta-induced settlement using photographs and engineering judgment, $S_{E,P}$, is estimated as

$$S_{E,P} = \frac{\sum_{i=1}^{n} A_{E,thick,i} * H_{E,thick,i} + \sum_{j=1}^{m} A_{E,thin,j} * H_{E,thin,j}}{A_T}$$

where $A_{E,thick,i}$ and $H_{E,thick,i}$ are the area and the height of a thick ejecta layer, respectively, $A_{E,thin,j}$ and $H_{E,thin,j}$ are the area and the height of a thin ejecta layer, respectively, and A_T is the total assessment area for a buffer being considered (Figure 1). The $A_{E,thick,i}$ and $A_{E,thin,i}$ are contained within the buffer.

Table 10: Ejecta-induced settlement estimates based on photographs.

Earthquake Event	10-m buffer		20-m buffer		50-m buffer	
	$S_{E,P,lower}$ (mm)	$S_{E,P,upper}$ (mm)	$S_{E,P,lower}$ (mm)	$S_{E,P,upper}$ (mm)	$S_{E,P,lower}$ (mm)	$S_{E,P,upper}$ (mm)
Sep-10	0	0	0	0	0	0
Feb-11	75	126	97	165	56	95
Jun-11	11	35	14	47	9	30
Dec-11	≈0	≈0	≈0	≈0	≈0	≈0

Note: $S_{E,P,lower}$ and $S_{E,P,upper}$ correspond to lower and upper estimates of $S_{E,P}$, respectively.

Table 11: Best final estimates of ejecta-induced settlement.

Earthquake Event	10-m buffer			20-m buffer			50-m buffer		
	$S_{E,L}$ (mm)	$S_{E,P}$ (mm)	$S_{E,final}$ (mm)	$S_{E,L}$ (mm)	$S_{E,P}$ (mm)	$S_{E,final}$ (mm)	$S_{E,L}$ (mm)	$S_{E,P}$ (mm)	$S_{E,final}$ (mm)
Sep-10	24±78	0	0	28±78	0	0	18±78	0	0
Feb-11	174±56	101±25	125±25	173±56	131±34	145±30	141±56	76±19	100±25
Jun-11	102±35	23±12	50±15	86±35	31±16	50±15	68±35	20±10	35±15
Dec-11	-83±71	≈0	<5	-78±71	≈0	<5	-63±71	≈0	<5

Notes: $S_{E,L}$ = Ejecta-induced settlement based on LiDAR data reported in Table 8; $S_{E,P}$ = Median ejecta-induced settlement for the range of values reported in Table 10; $S_{E,final}$ = Best final estimate of ejecta-induced settlement rounded to the nearest 5 mm; Final plus/minus values are also rounded to the nearest 5 mm.

Note 5: $S_{E,final}$ is a weighted average of $S_{E,L}$ and $S_{E,P}$ with weights of 1/3 and 2/3, respectively. The uncertainty associated with $S_{E,final}$ is also a weighted average of uncertainties associated with $S_{E,L}$ and $S_{E,P}$ with the same weights of 1/3 and 2/3, respectively. The weights are based on the LiDAR error bands, LPI prediction error (Maurer et al. 2014[3]), and completeness of visual evidence (i.e., ground and aerial photographs and EQC LDAT property inspection reports for the site). Shirley Intermediate School is located in the apparent zone of higher/lower ground surface subsidence compared to the adjacent areas to the west and east for the Sep-10/Feb-11 earthquake (i.e., the underestimate of the ground surface elevation by the Sep-10 LiDAR survey). The site is also in the zone of slight to moderate LPI underprediction of liquefaction severity for Feb-11 EQ. The LPI prediction of liquefaction severity for Sep-10 EQ is accurate. There is high-resolution aerial photograph for the site but no ground photographs or LDAT property reports for the site. The ground photograph for the neighboring area is available from the residents' report mentioned in Note 4.

Summary 1: The best estimate of the ejecta-induced free-field ground settlement at the Shirley Intermediate School site for the SEP 2010, FEB 2011, JUN 2011, and DEC 2011 earthquake is 0 mm, 125±25 mm, 50±15 mm, and <5 mm, respectively.

[3] Maurer, B. W., Green, R. A., Cubrinovski, M., & Bradley, B. A. (2014). Evaluation of the Liquefaction Potential Index for Assessing Liquefaction Hazard in Christchurch, New Zealand. *Journal of Geotechnical and Geoenvironmental Engineering*, 140(7), 04014032-1-11. doi:10.1061/(asce)gt.1943-5606.0001117

Figure 5: Location of the site.

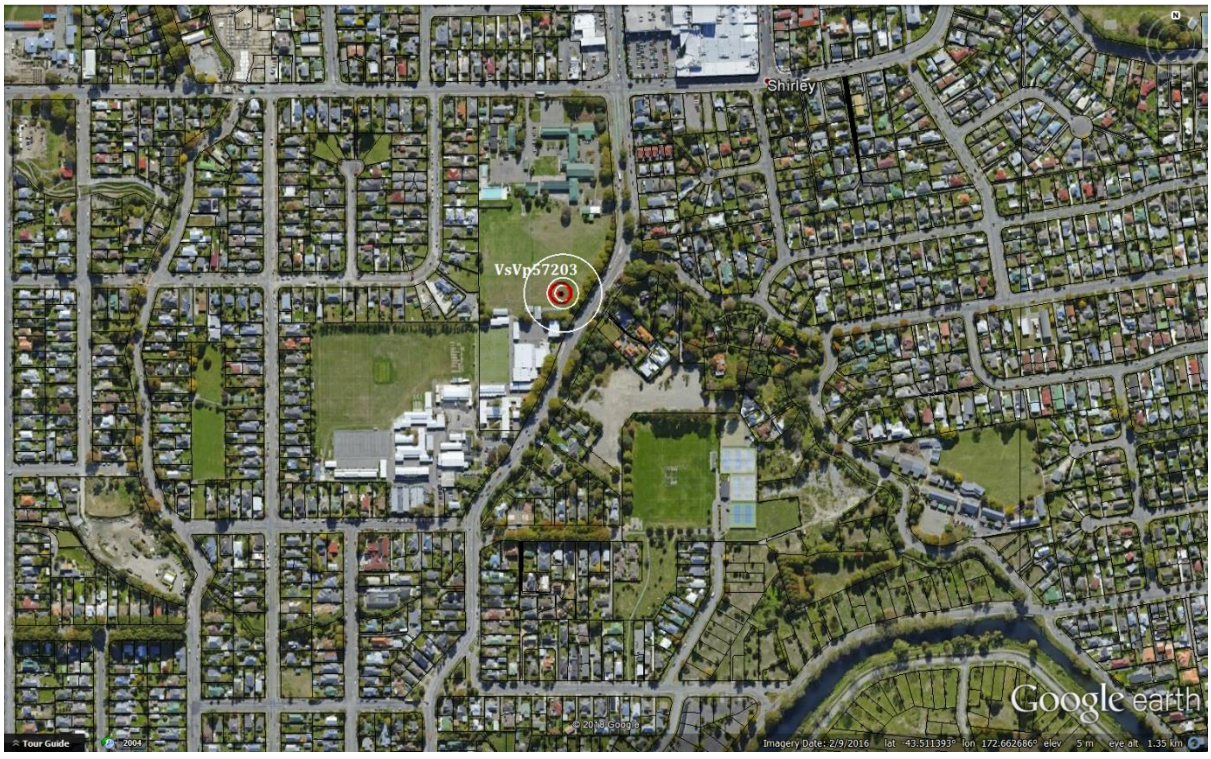

Figure 6: Position of the site relative to nearby buildings, vegetation, and free-face features.

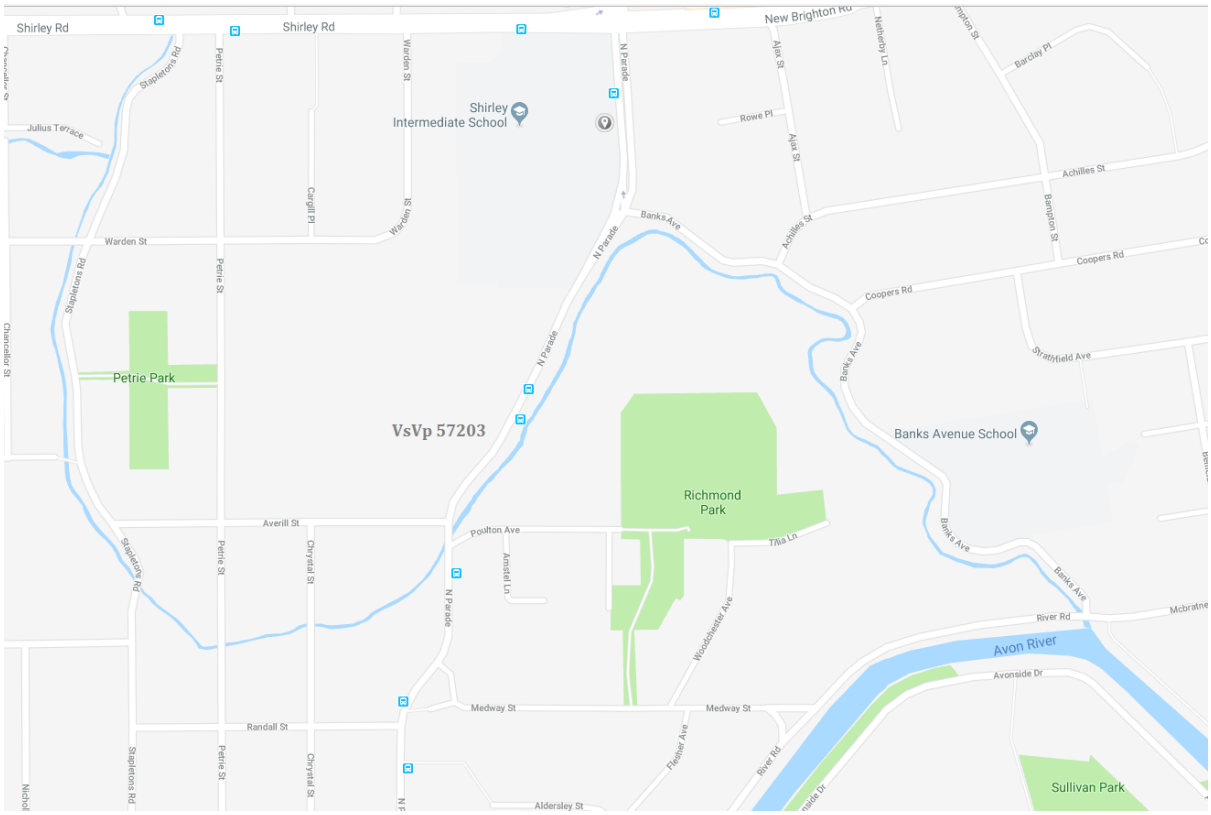

Figure 7: Position of the site relative to the creek.

Figure 8: Street view of the flat land.

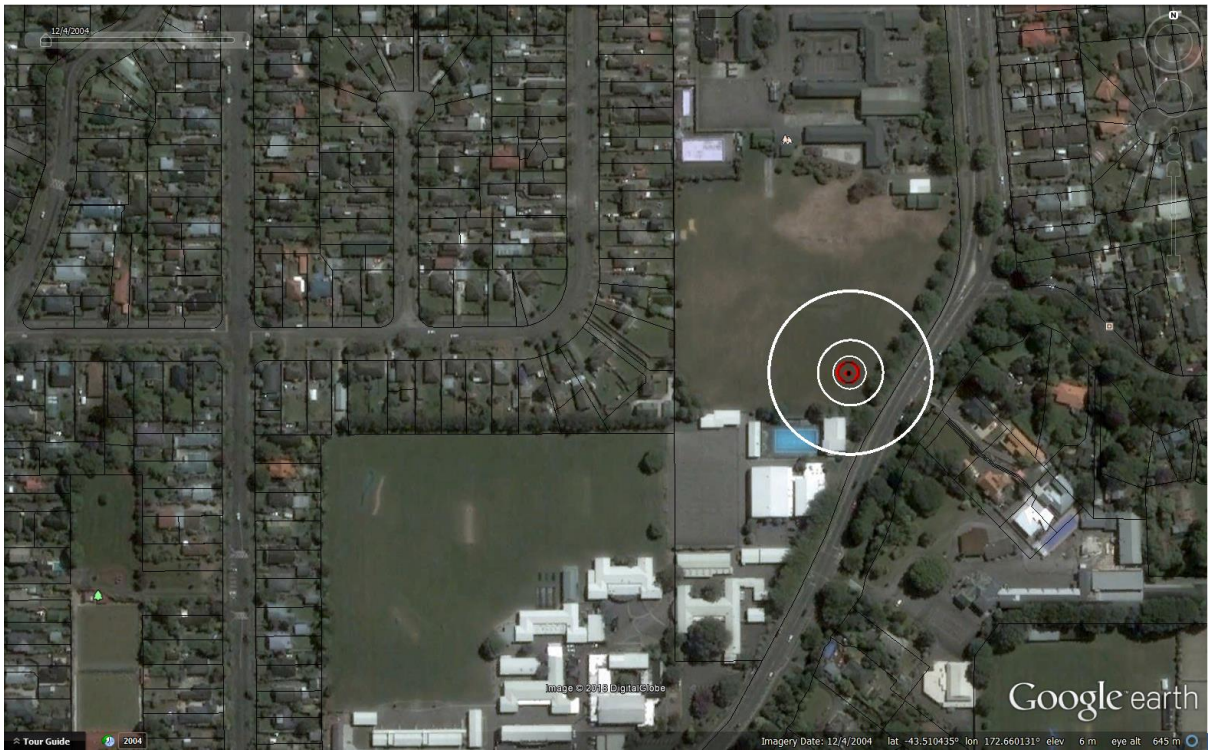

Figure 9: Aerial photograph of the site taken in Dec 2004.

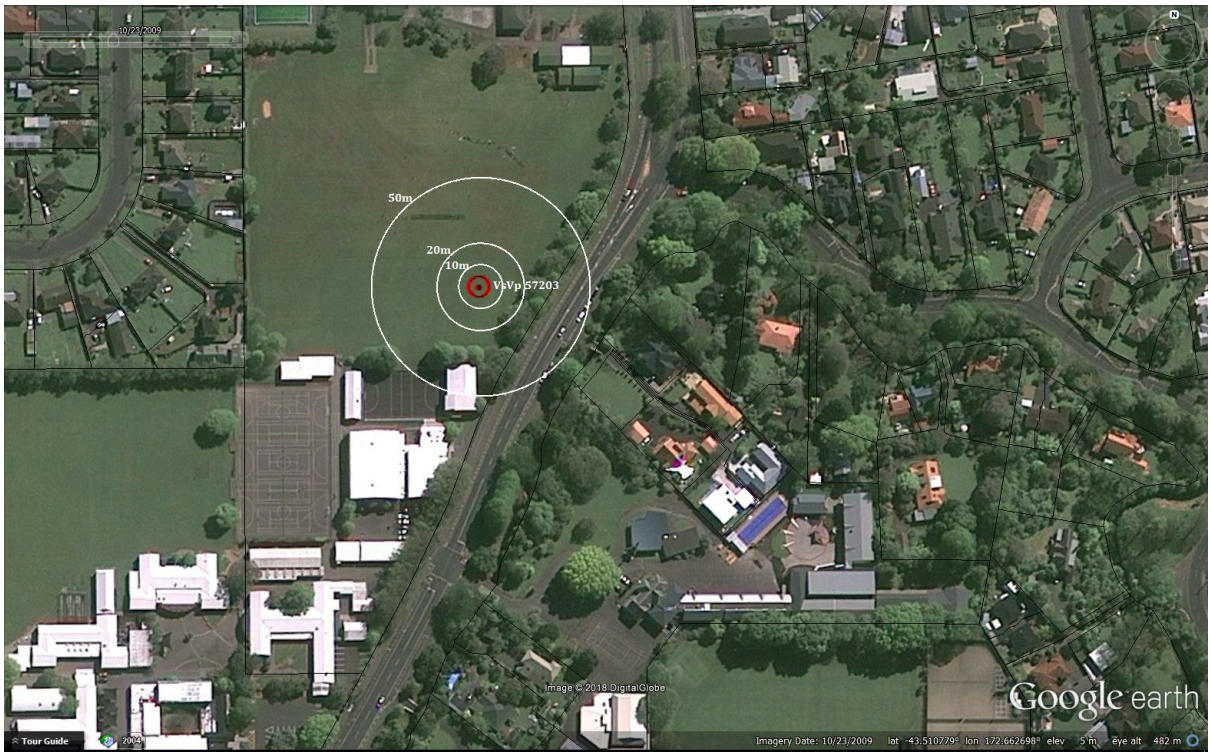

Figure 10: Aerial photograph of the site taken in Oct 2009.

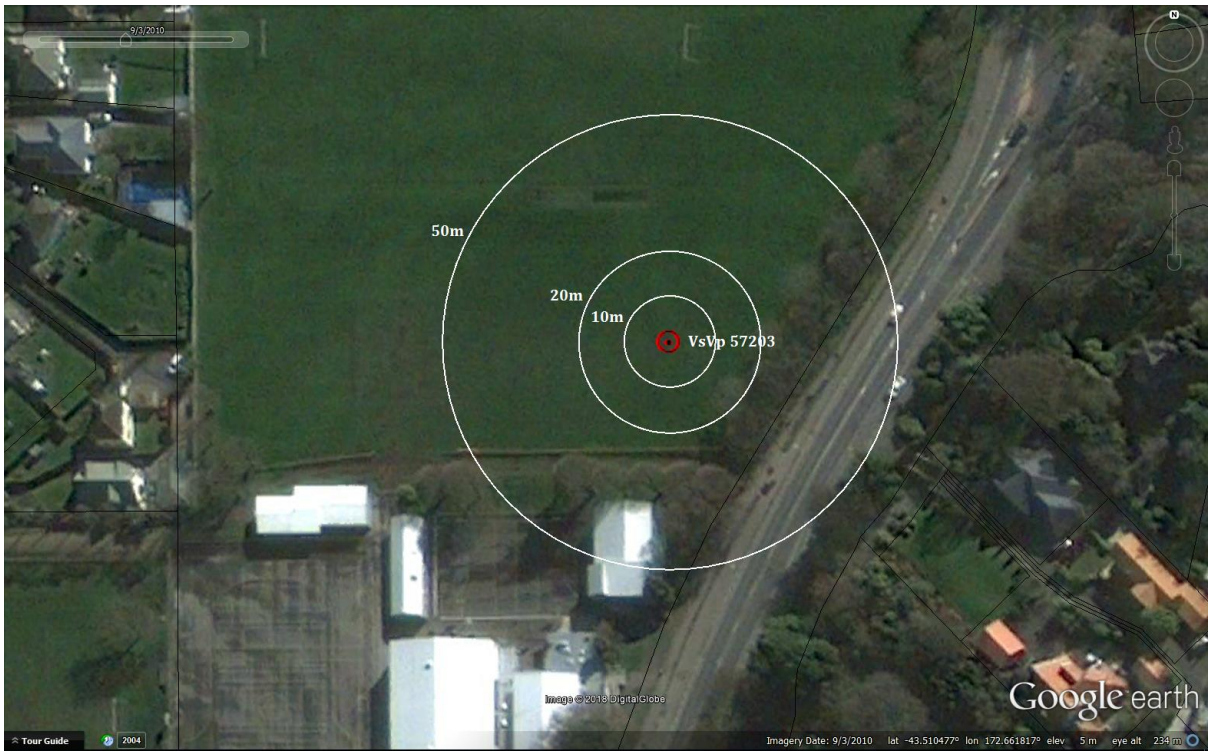

Figure 11: Aerial photograph of the site taken in Sep 2010.

Figure 12: Aerial photograph of the site taken in Nov 2015.

Figure 13: Aerial photograph of the site taken on Sep 4, 2010.

Figure 14: Aerial photograph of the site taken on Feb 24, 2011.

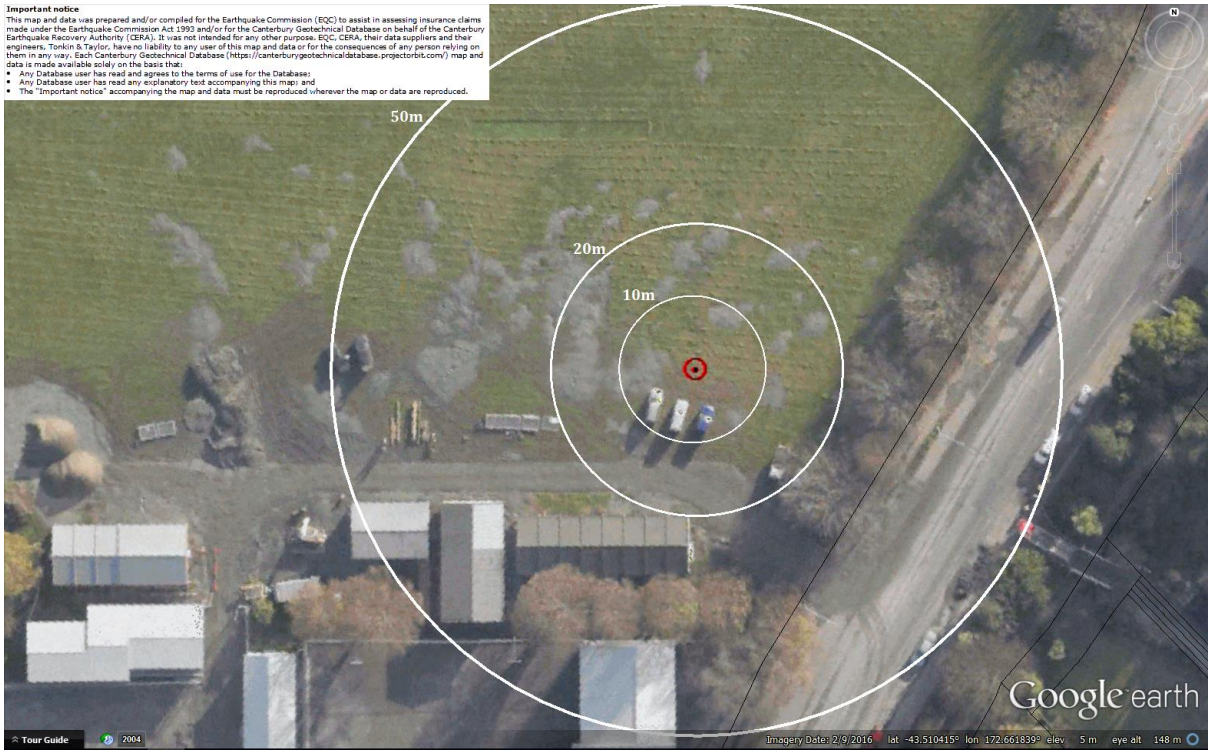

Figure 15: Aerial photograph of the site taken on June 14-15, 2011.

Figure 16: Aerial photograph of the site taken on June 16, 2011.

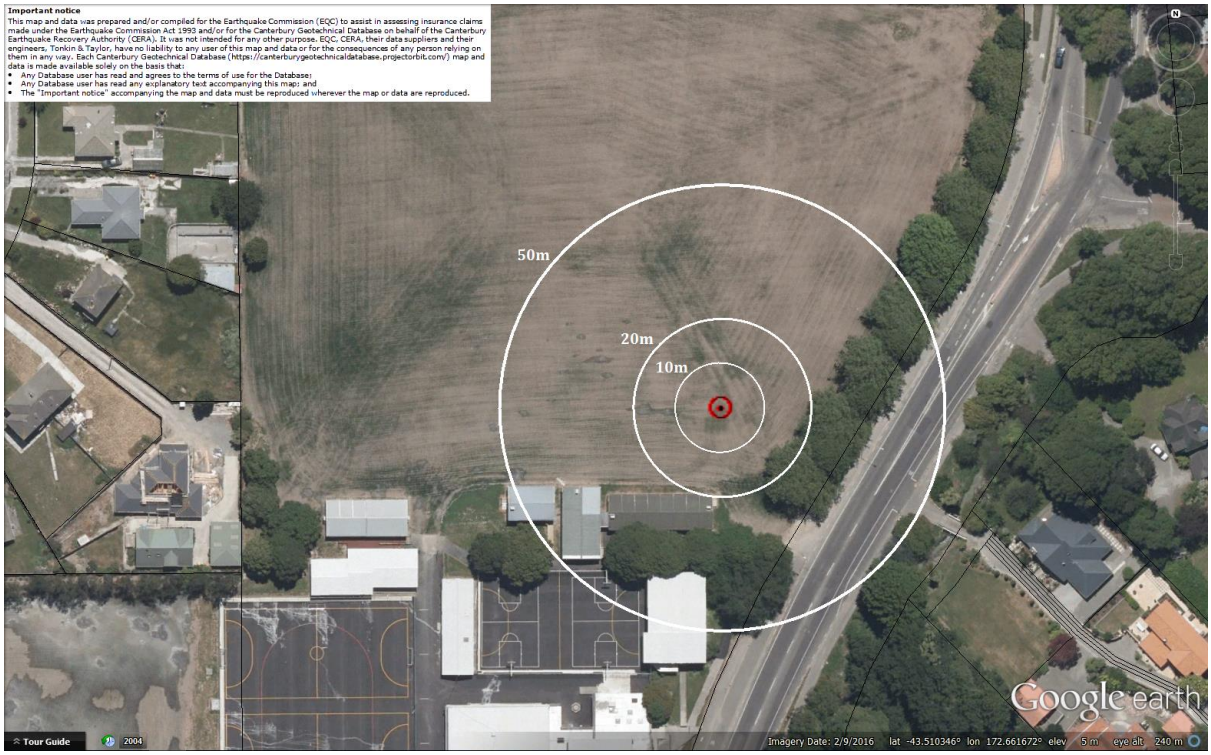

Figure 17: Aerial photograph of the site taken on Dec 24, 2012.

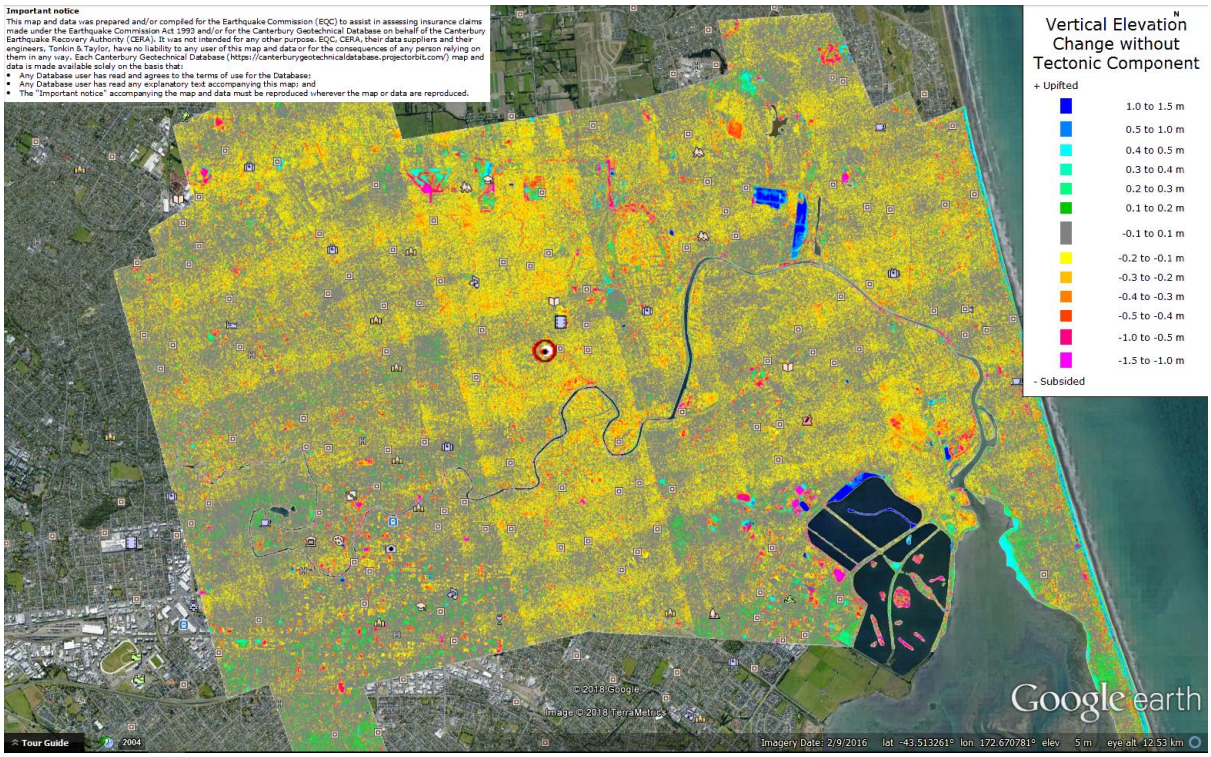

Figure 18: Vertical Ground Movements (Surface – Tectonic) for Sep 2010 Earthquake – the site is in the apparent zone of overestimated ground surface subsidence.

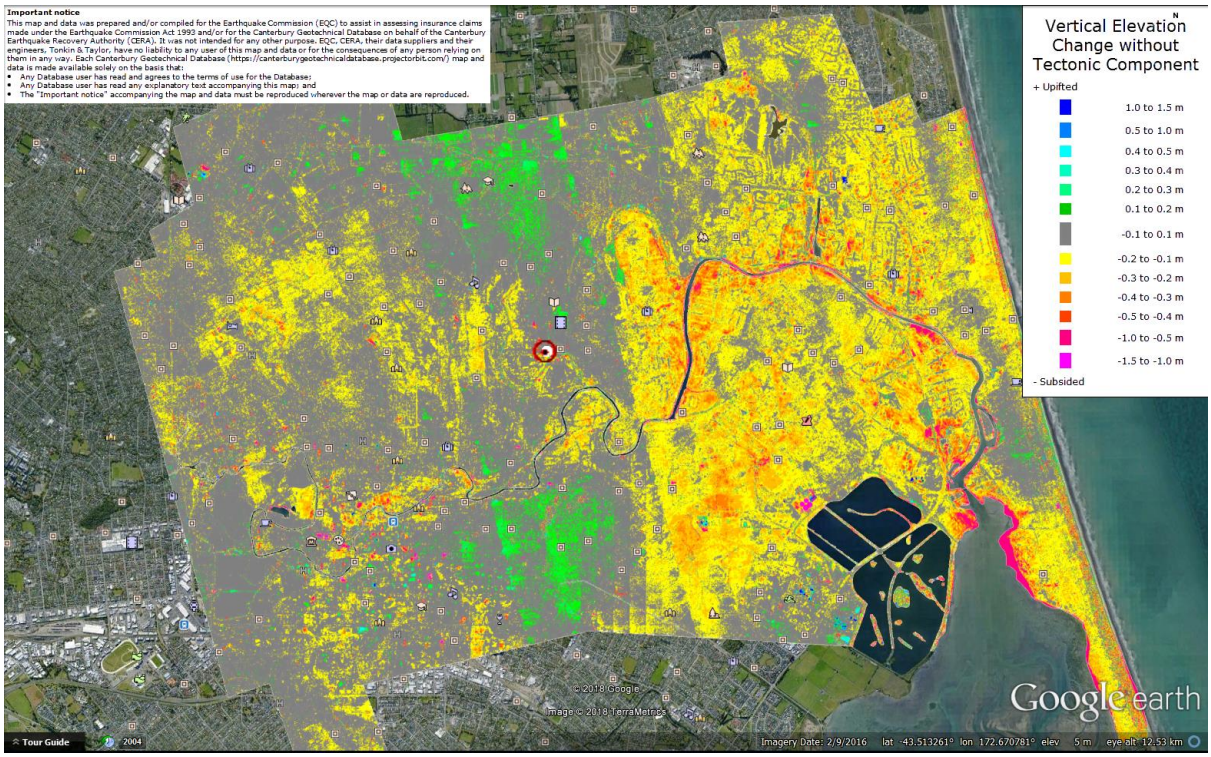

Figure 19: Vertical Ground Movements (Surface – Tectonic) for Feb 2011 Earthquake – the site is in the apparent zone of underestimated ground surface subsidence.

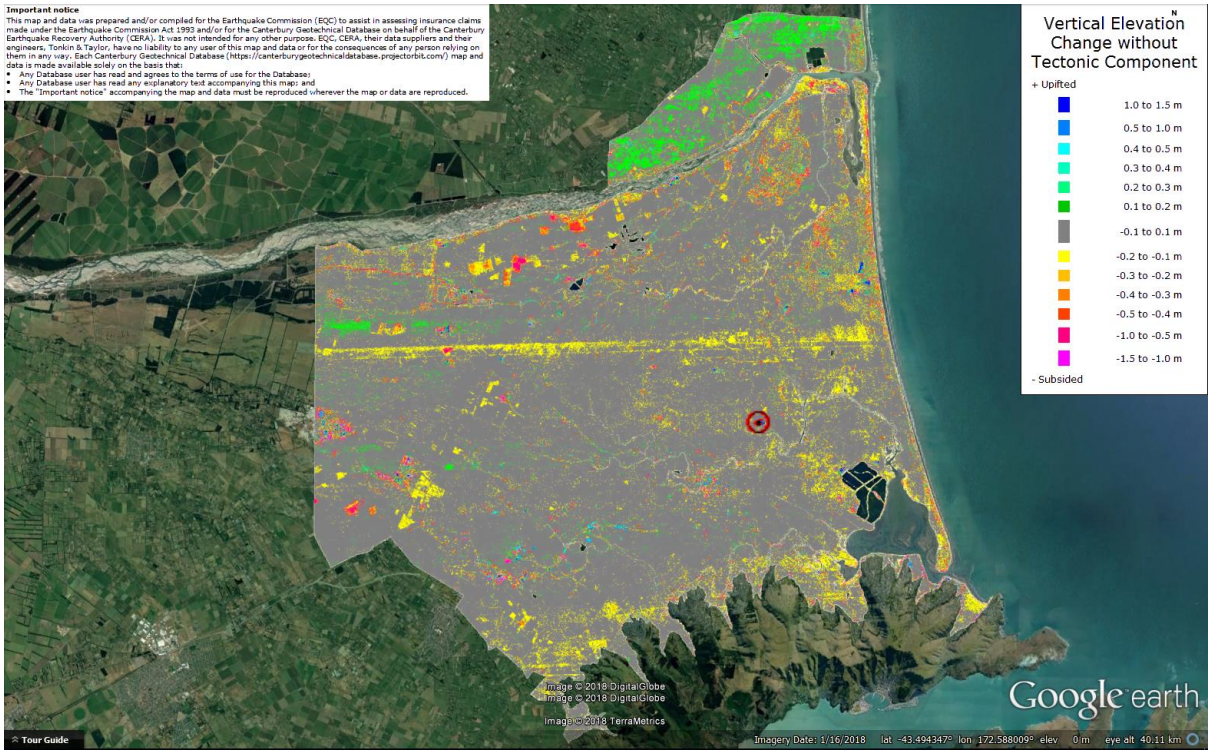

Figure 20: Vertical Ground Movements (Surface – Tectonic) for June 2011 Earthquake – the site is not in the apparent zone of overestimated or underestimated ground surface subsidence.

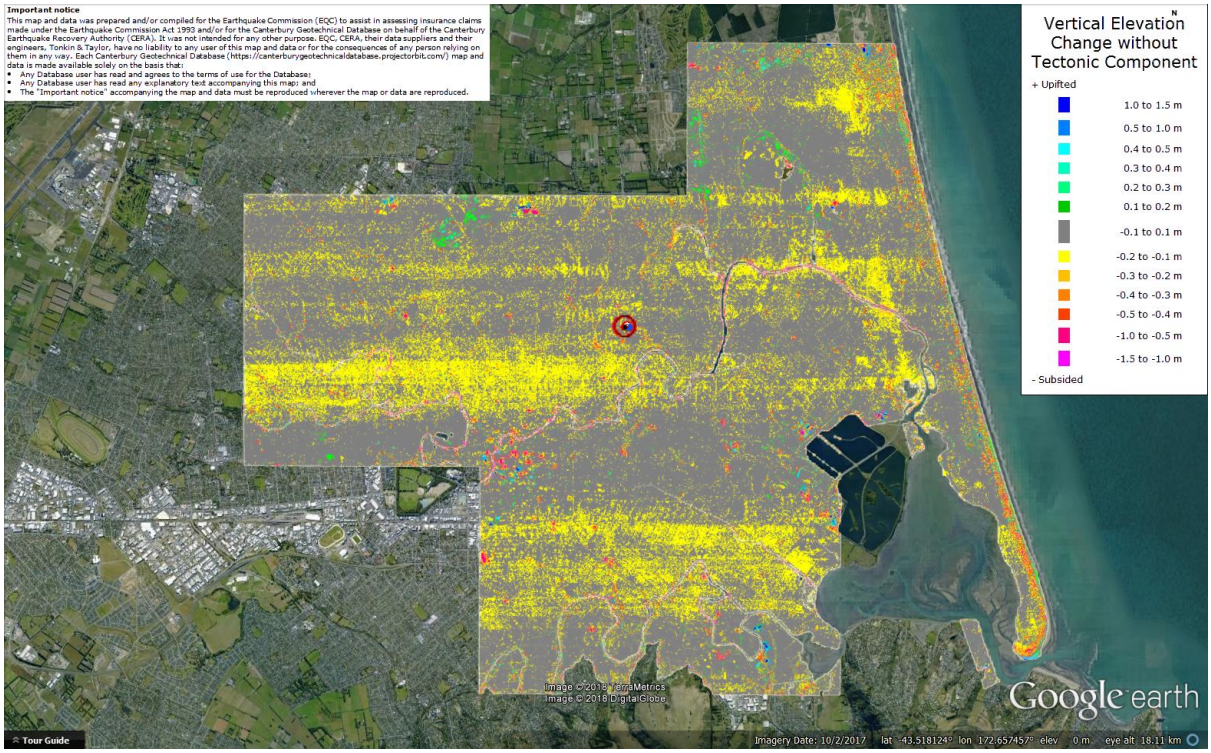

Figure 21: Vertical Ground Movements (Surface – Tectonic) for Dec 2011 Earthquake – the site is not in the apparent zone of overestimated or underestimated ground surface subsidence.

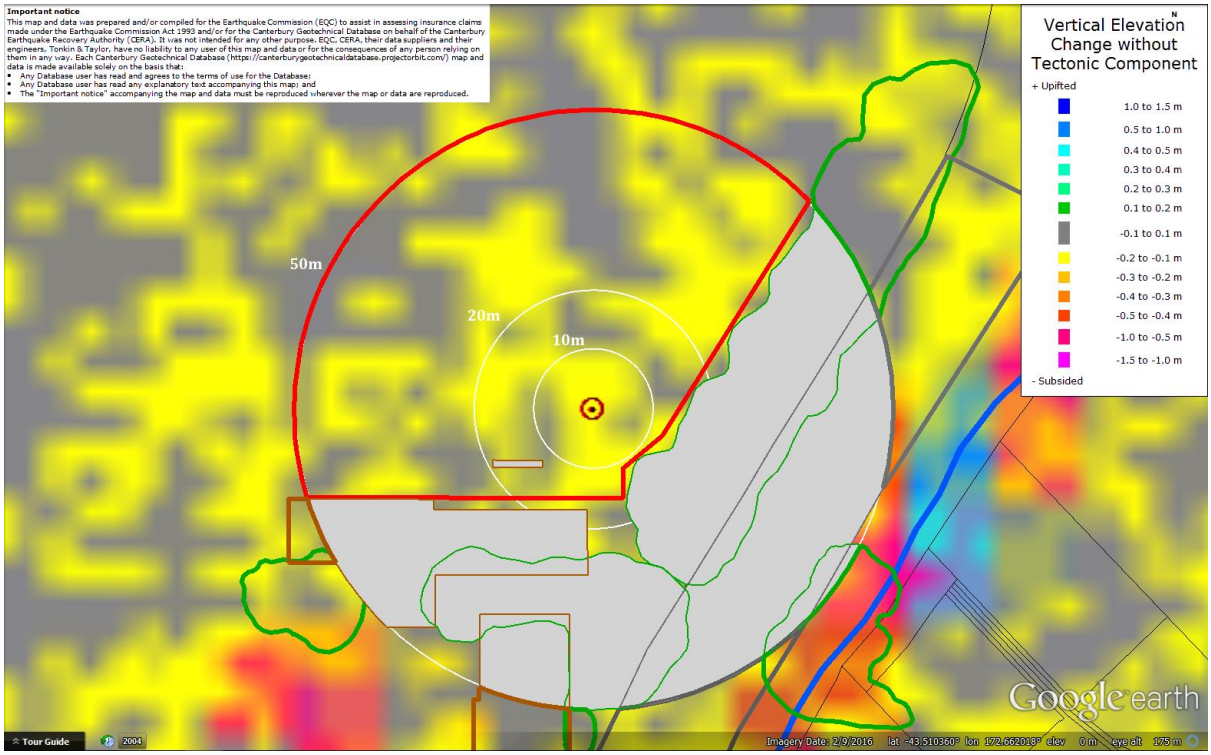

Figure 22: Ground surface subsidence without tectonic component for Sep 2010 Earthquake according to the LiDAR DEM.

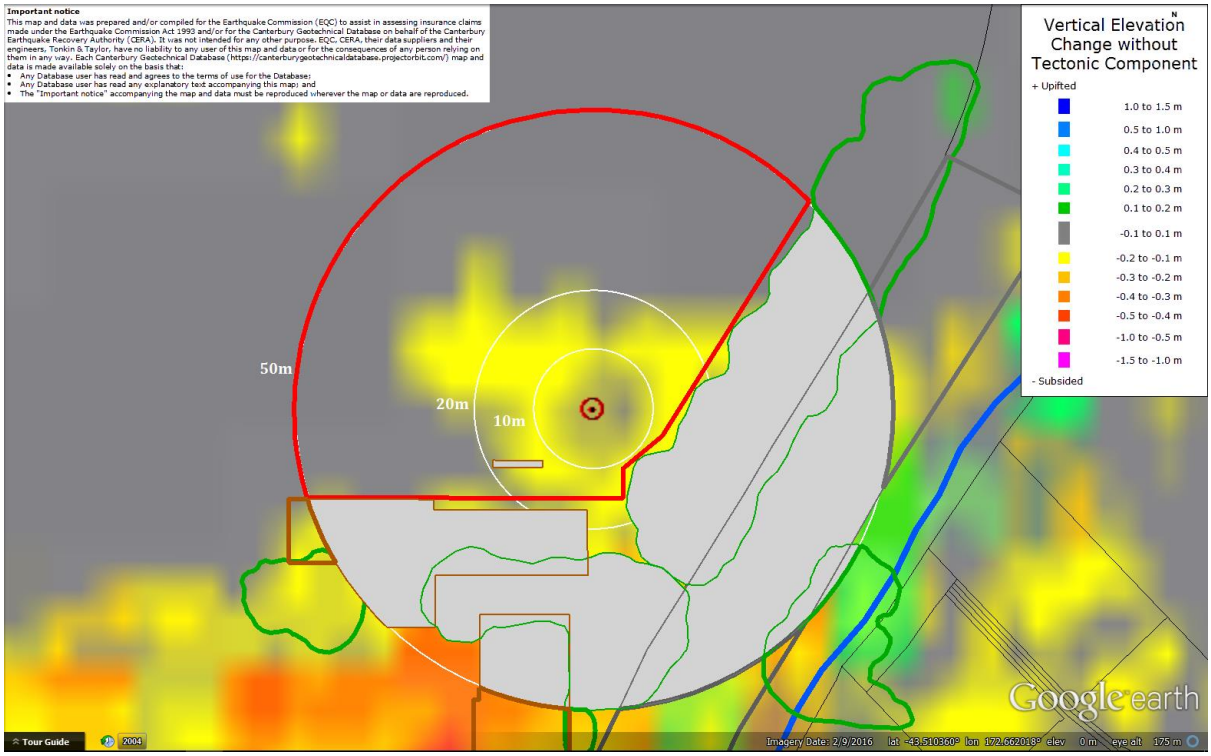

Figure 23: Ground surface subsidence without tectonic component for Feb 2011 Earthquake according to the LiDAR DEM.

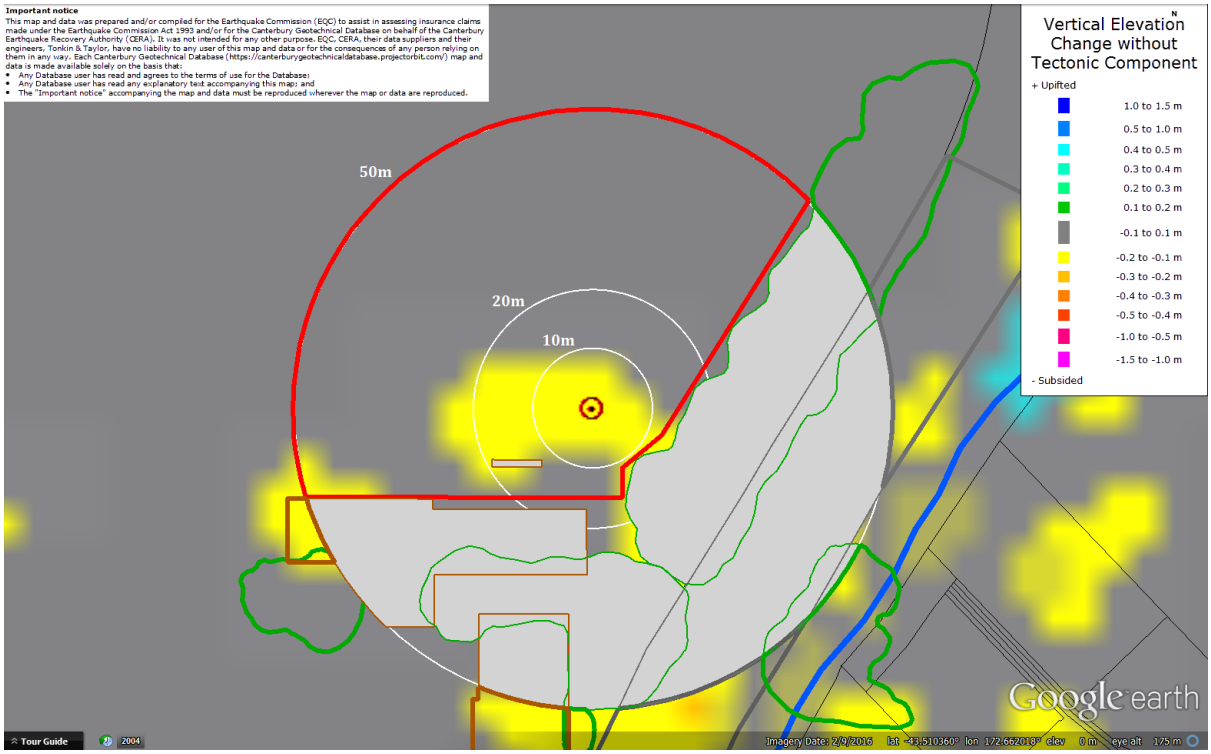

Figure 24: Ground surface subsidence without tectonic component for Jun 2011 Earthquake according to the LiDAR DEM.

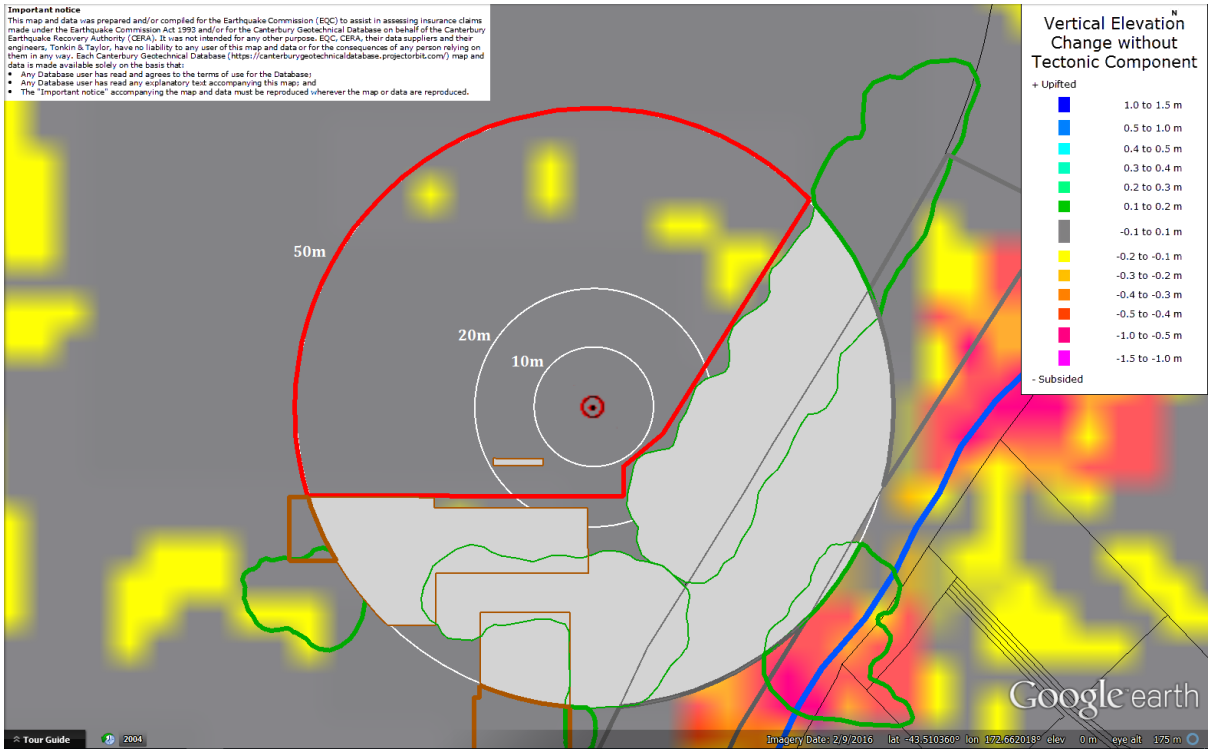

Figure 24: Ground surface subsidence without tectonic component for Dec 2011 Earthquake according to the LiDAR DEM.

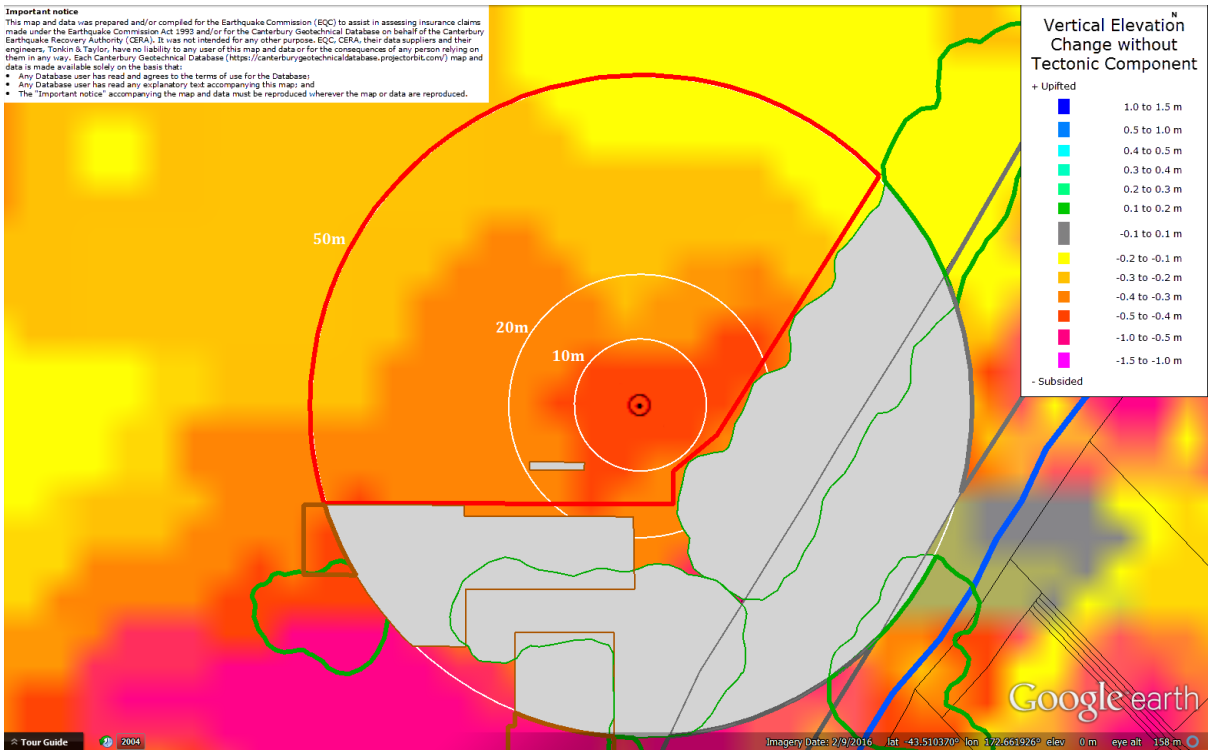

Figure 25: Ground surface subsidence without tectonic component for Canterbury Earthquake Sequence according to the LiDAR DEM.

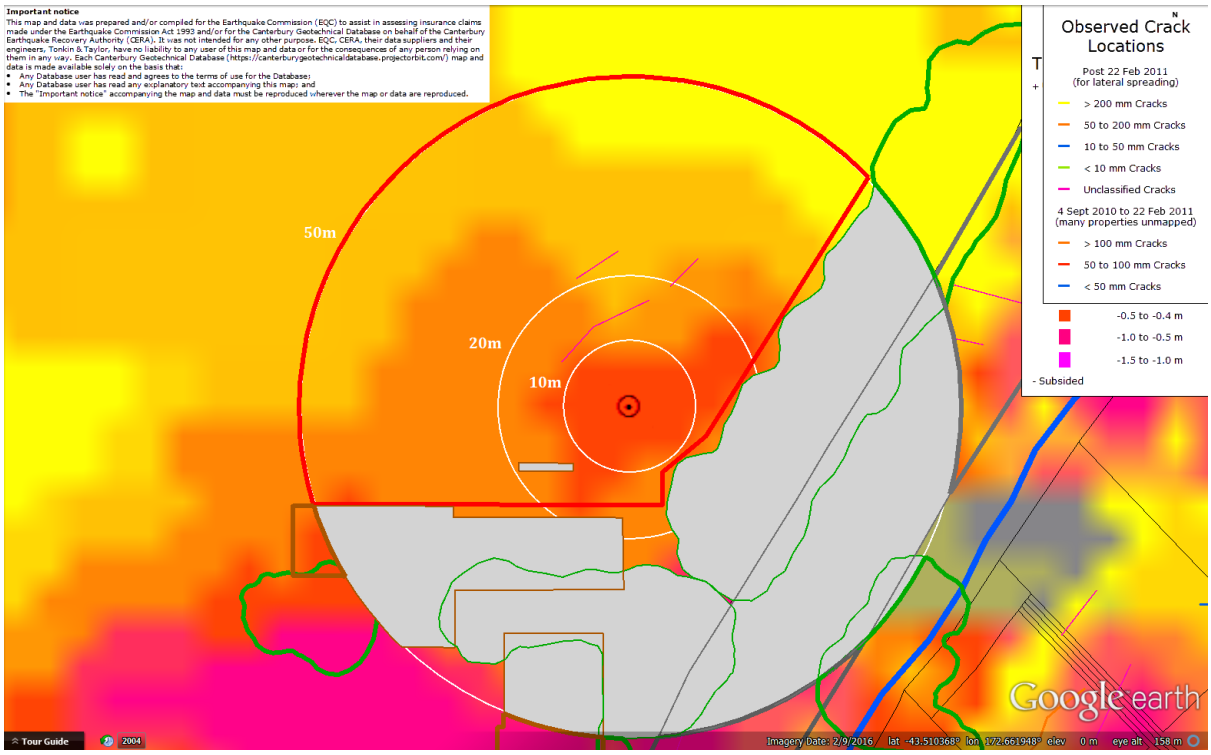

Figure 26: Absence of ground cracks indicating no lateral spreading for Canterbury Earthquake Sequence.

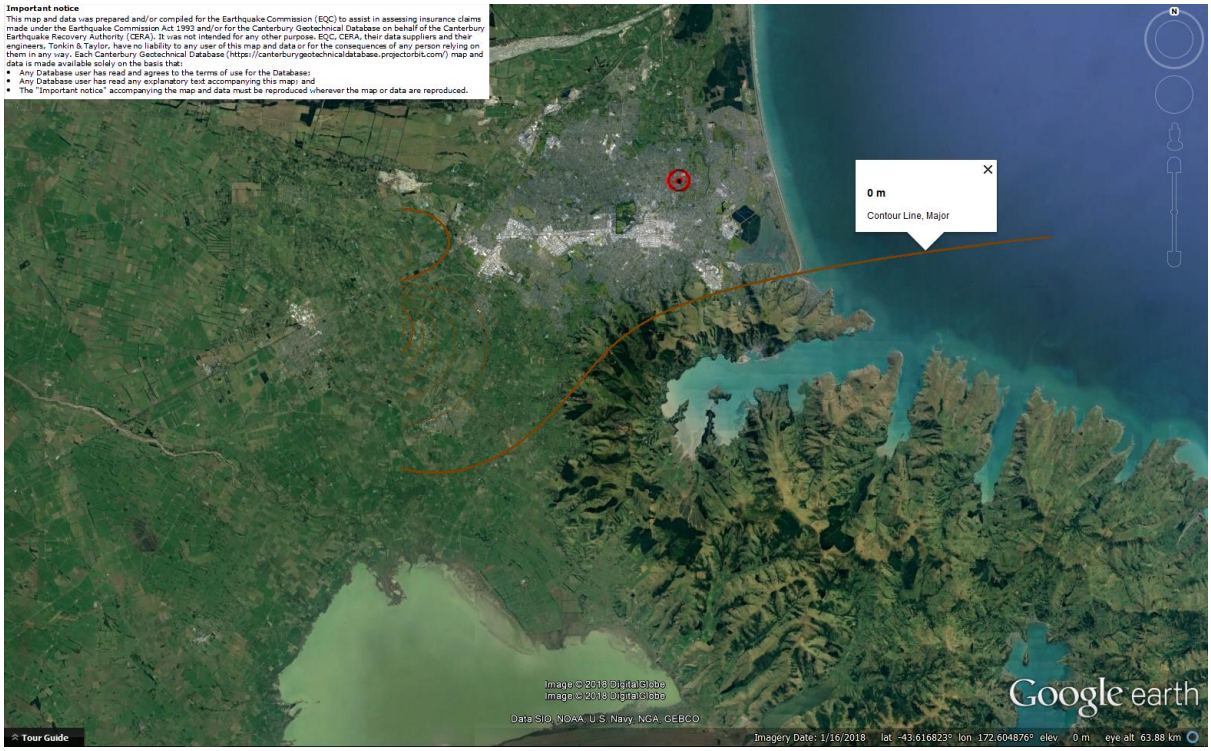

Figure 27: Vertical tectonic movements for Sep 2010 Earthquake.

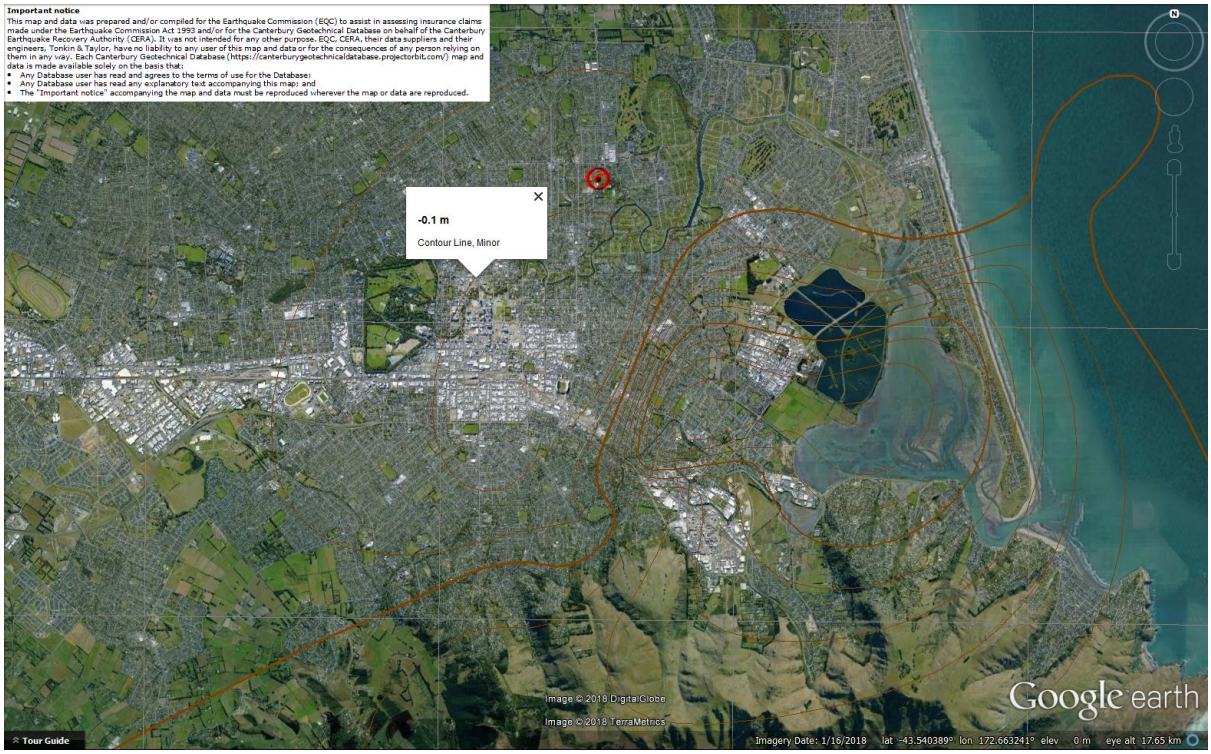

Figure 28: Vertical tectonic movements for Feb 2011 Earthquake.

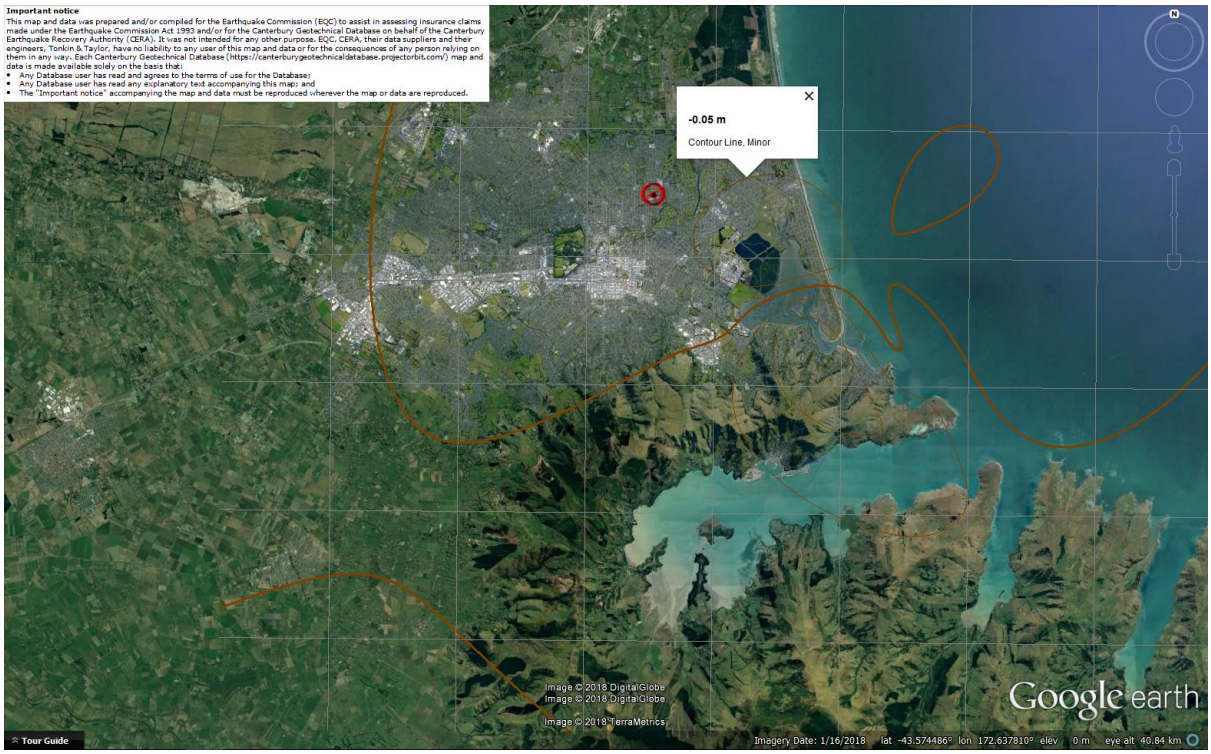

Figure 29: Vertical tectonic movements for June 2011 Earthquake.

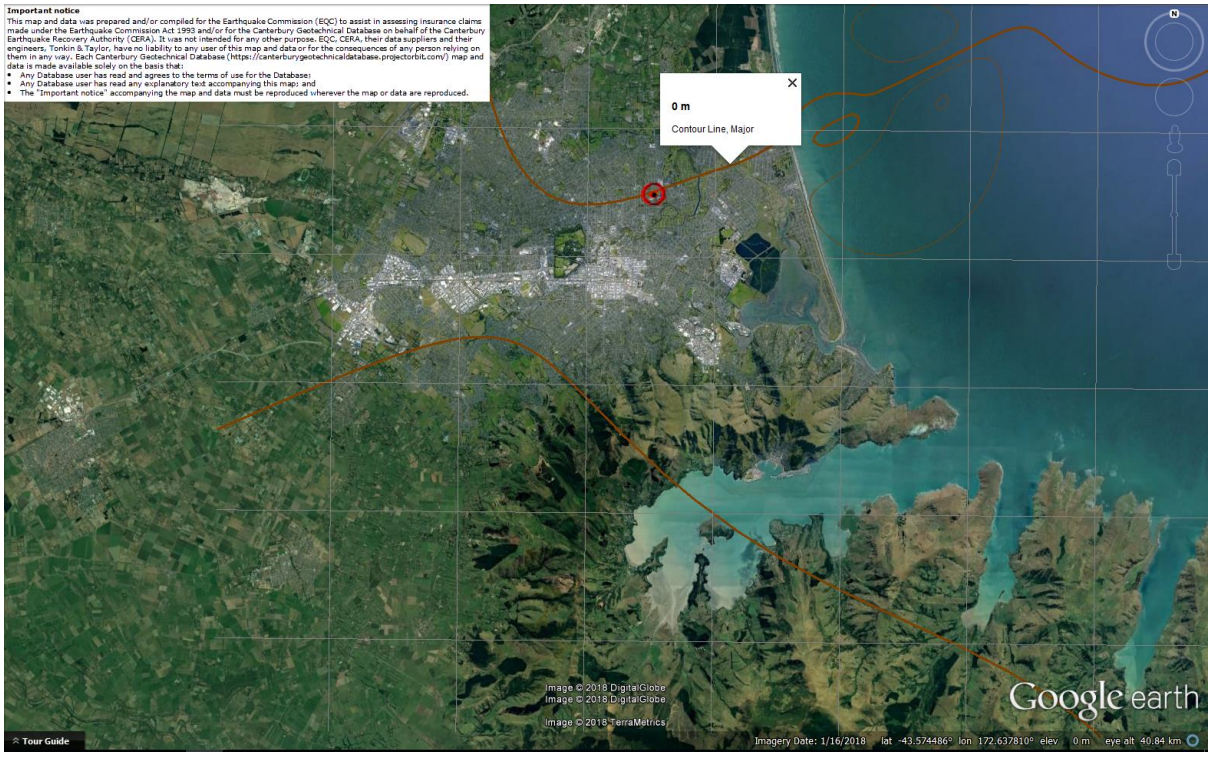

Figure 30: Vertical tectonic movements for Dec 2011 Earthquake.

Figure 31: Vertical tectonic movements for Canterbury Earthquake Sequence.

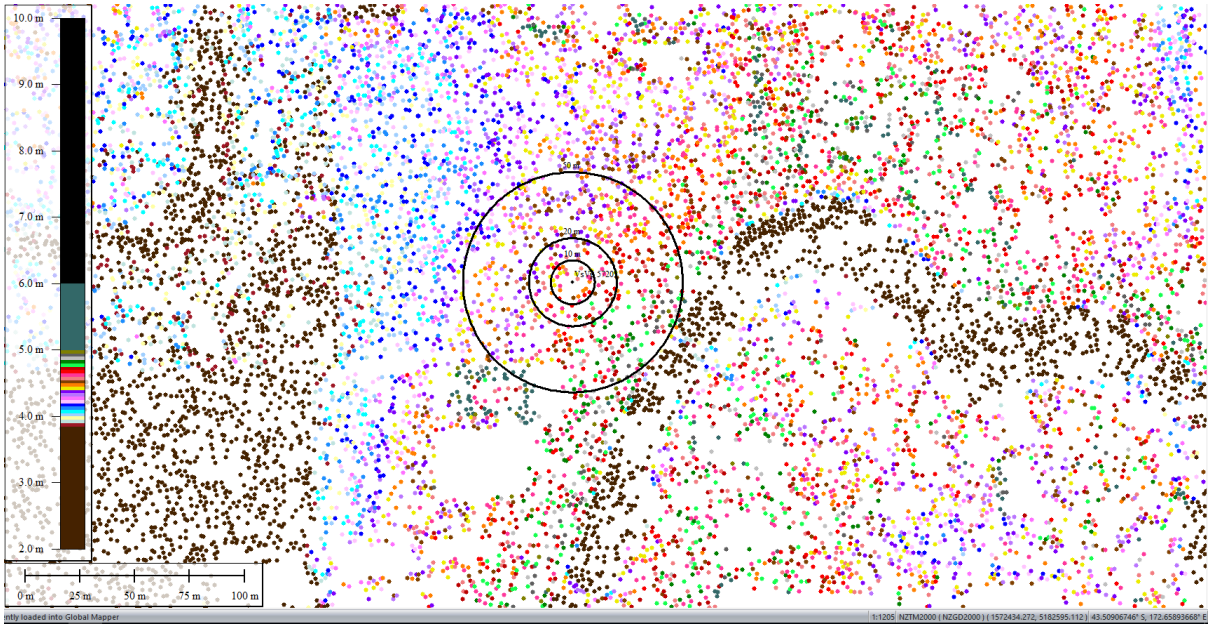

Figure 32: Jul 2003 LiDAR survey.

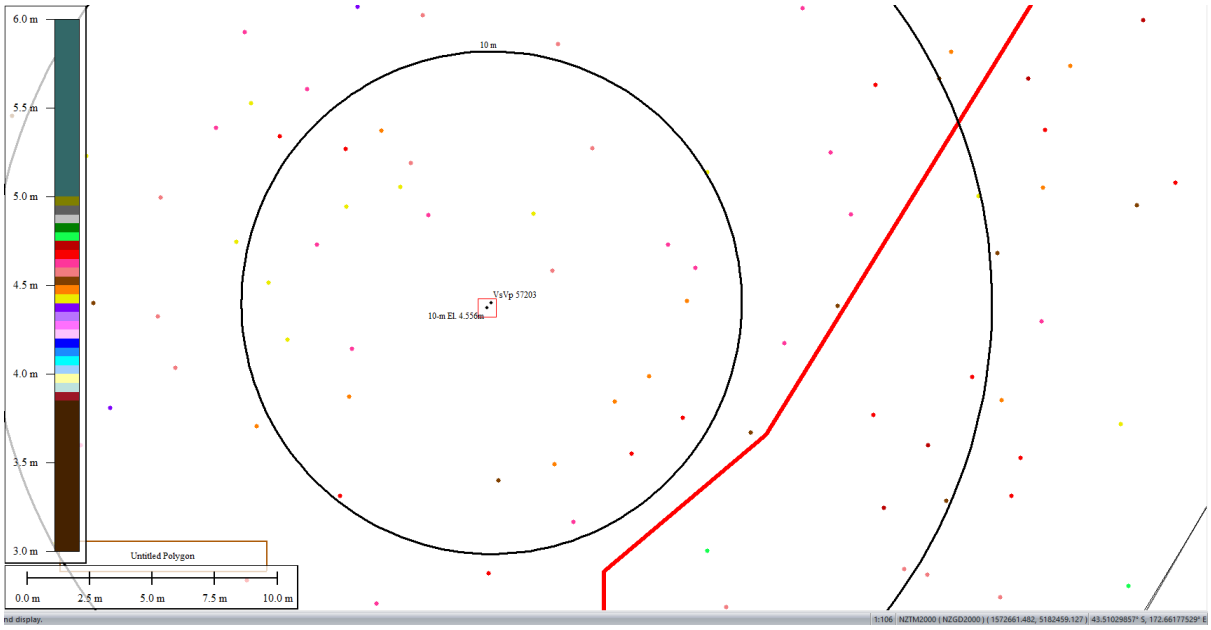

Figure 33: Ground surface elevation averaged over 10-m buffer for Jul 2003 LiDAR survey.

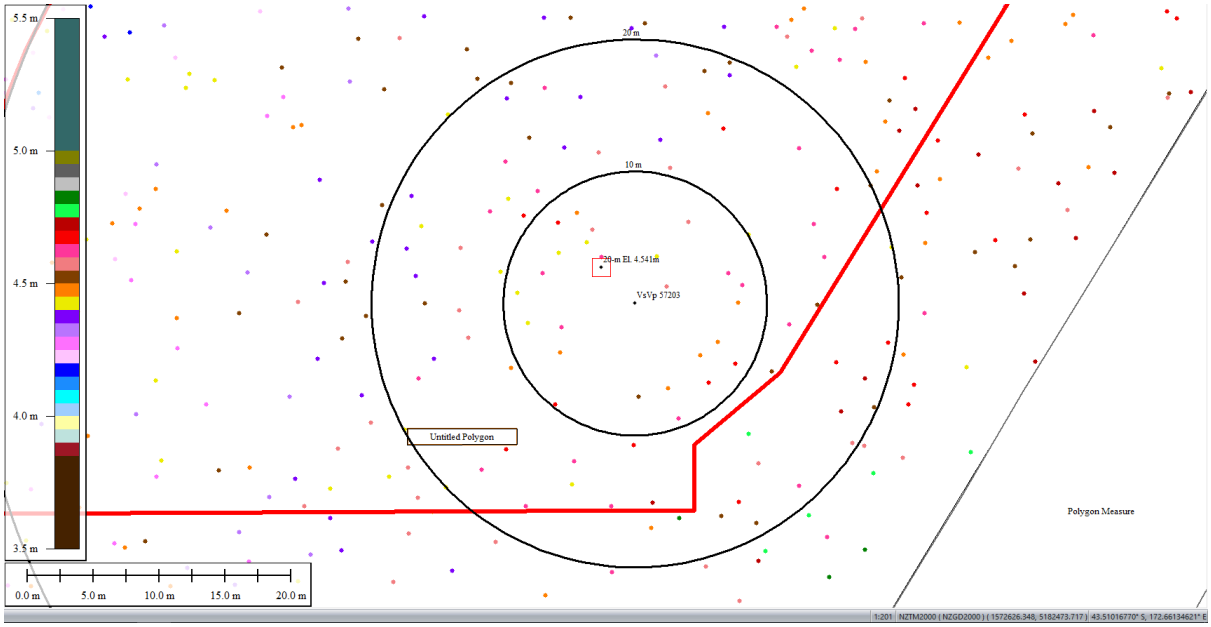

Figure 34: Ground surface elevation averaged over 20-m buffer for Jul 2003 LiDAR survey.

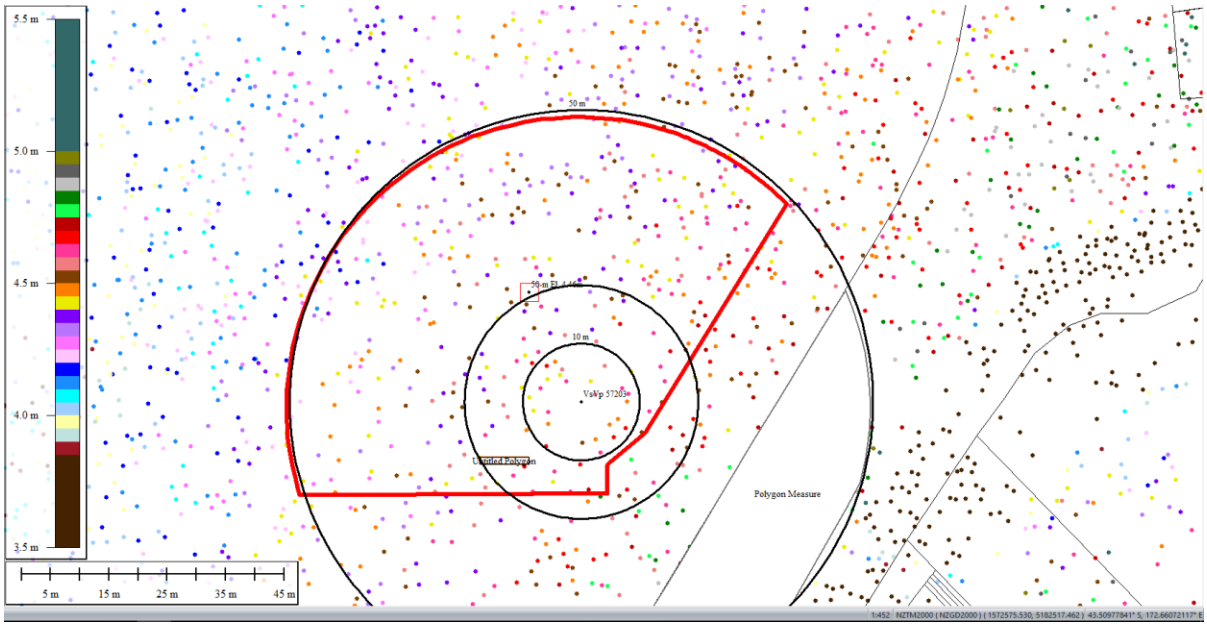

Figure 35: Ground surface elevation averaged over 50-m buffer for Jul 2003 LiDAR survey.

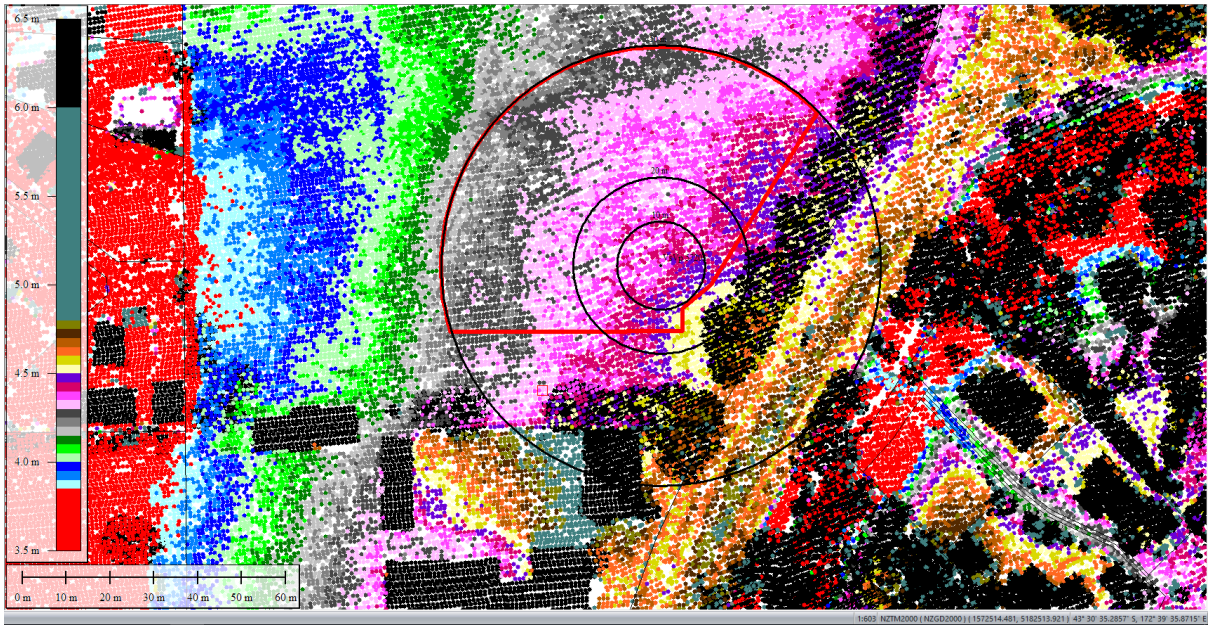

Figure 36: Sep 5, 2010 LiDAR survey.

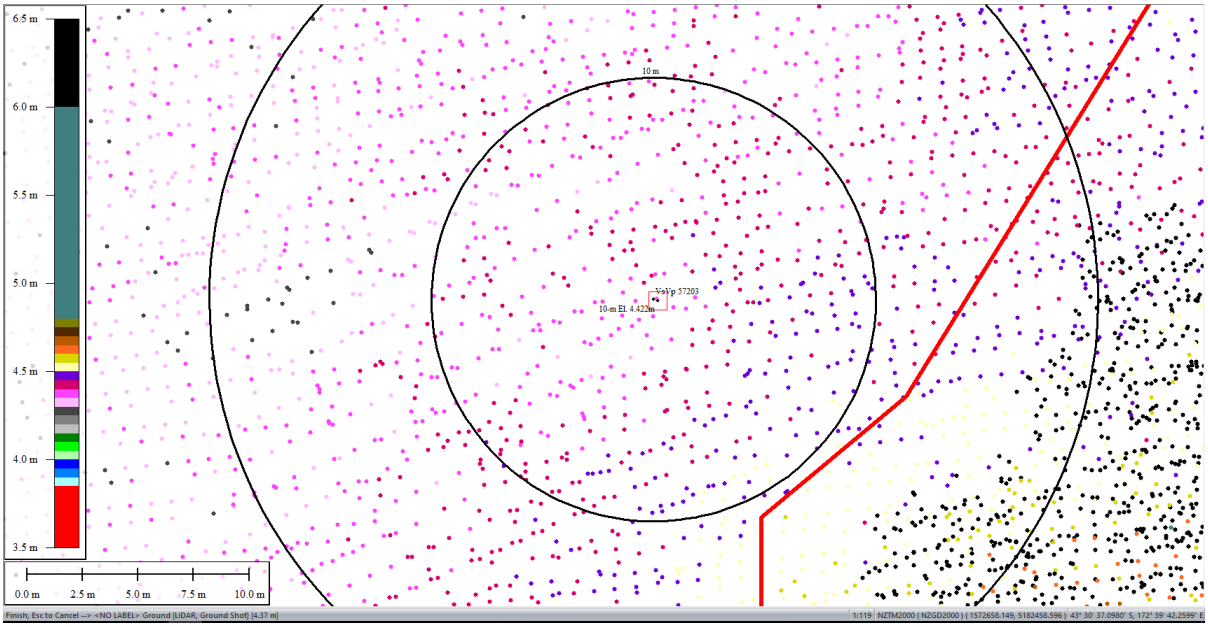

Figure 37: Ground surface elevation averaged over 10-m buffer for Sep 5, 2010 LiDAR survey.

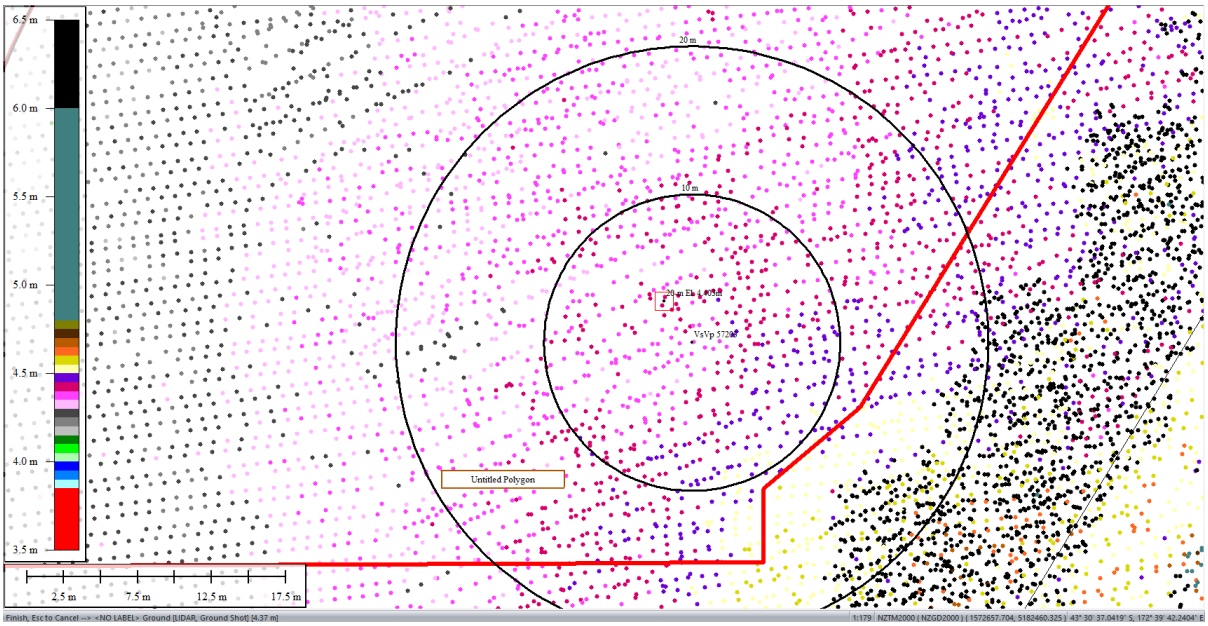

Figure 38: Ground surface elevation averaged over 20-m buffer for Sep 5, 2010 LiDAR survey.

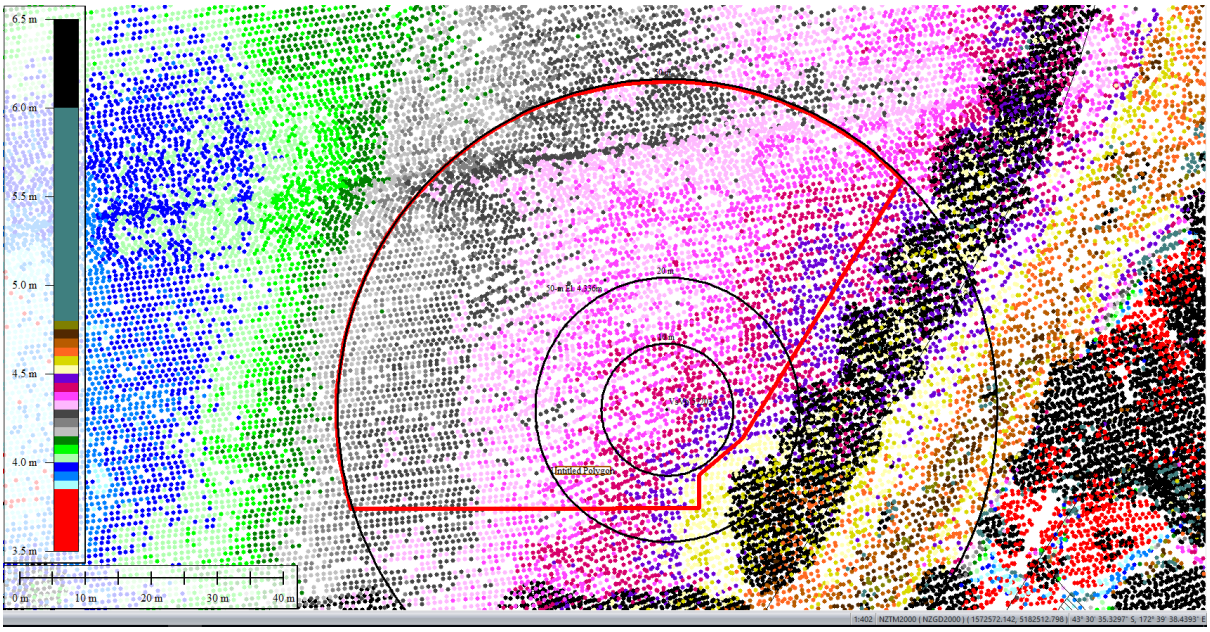

Figure 39: Ground surface elevation averaged over 50-m buffer for Sep 5, 2010 LiDAR survey.

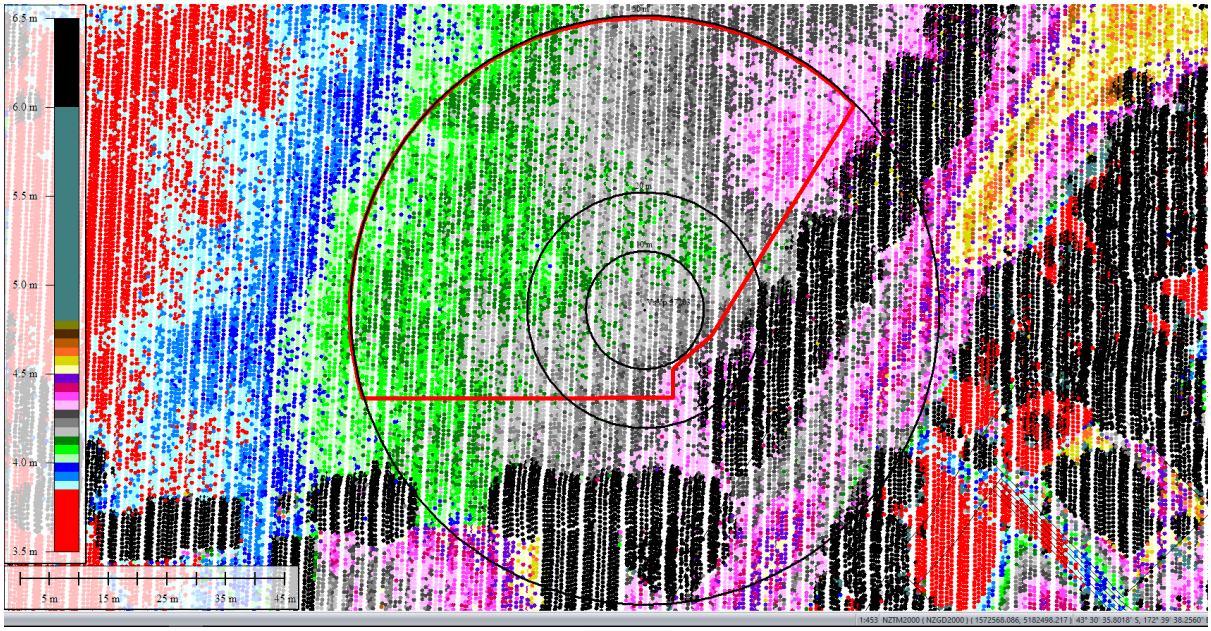

Figure 40: Mar 2011 LiDAR survey.

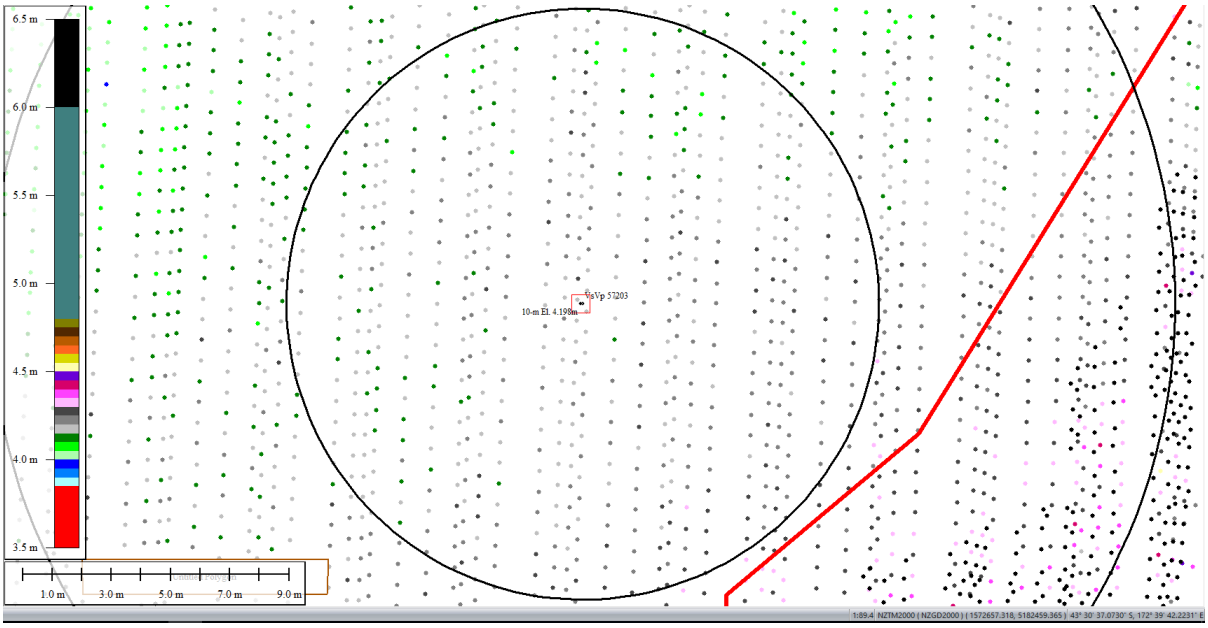

Figure 41: Ground surface elevation averaged over 10-m buffer for Mar 2011 LiDAR survey.

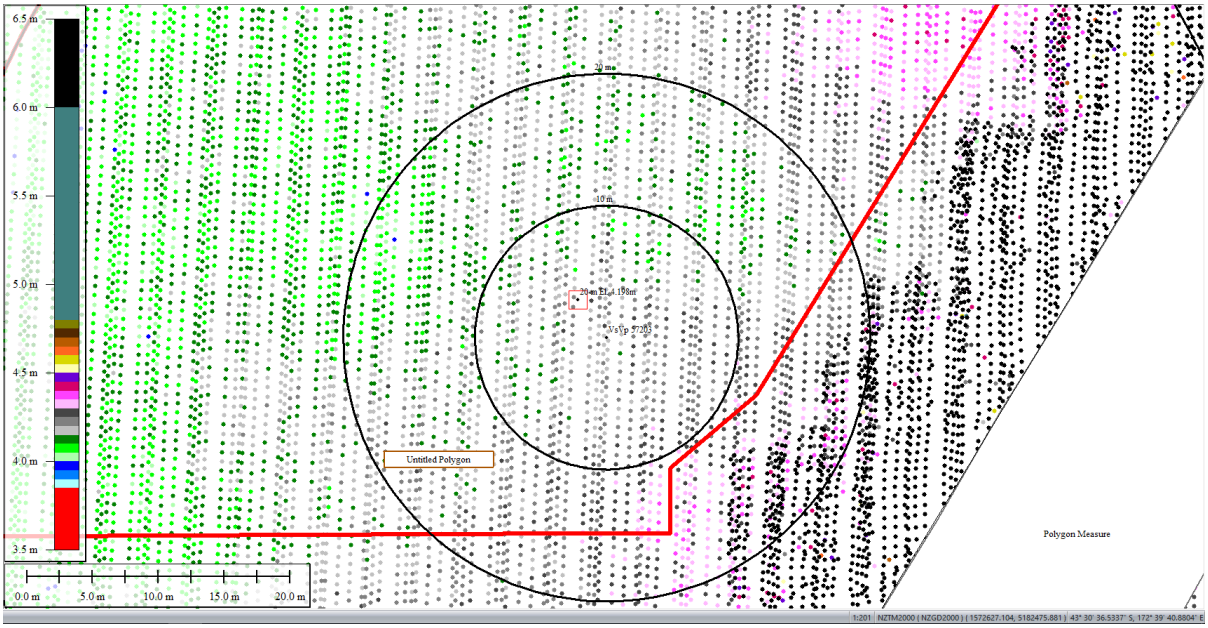

Figure 42: Ground surface elevation averaged over 20-m buffer for Mar 2011 LiDAR survey.

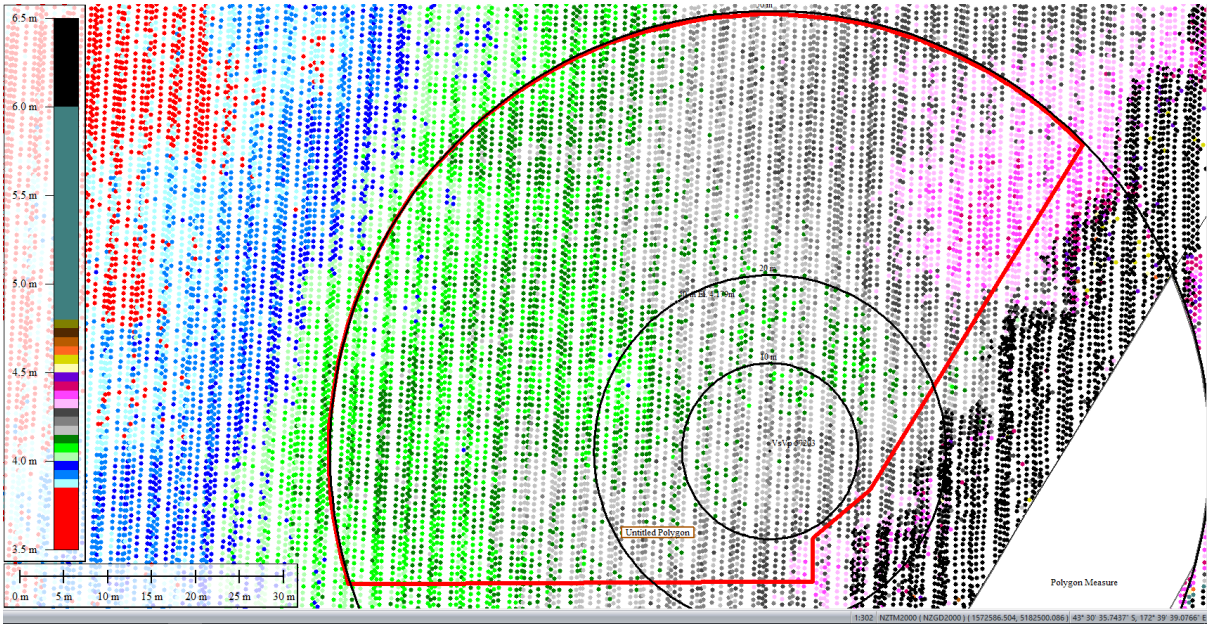

Figure 43: Ground surface elevation averaged over 50-m buffer for Mar 2011 LiDAR survey.

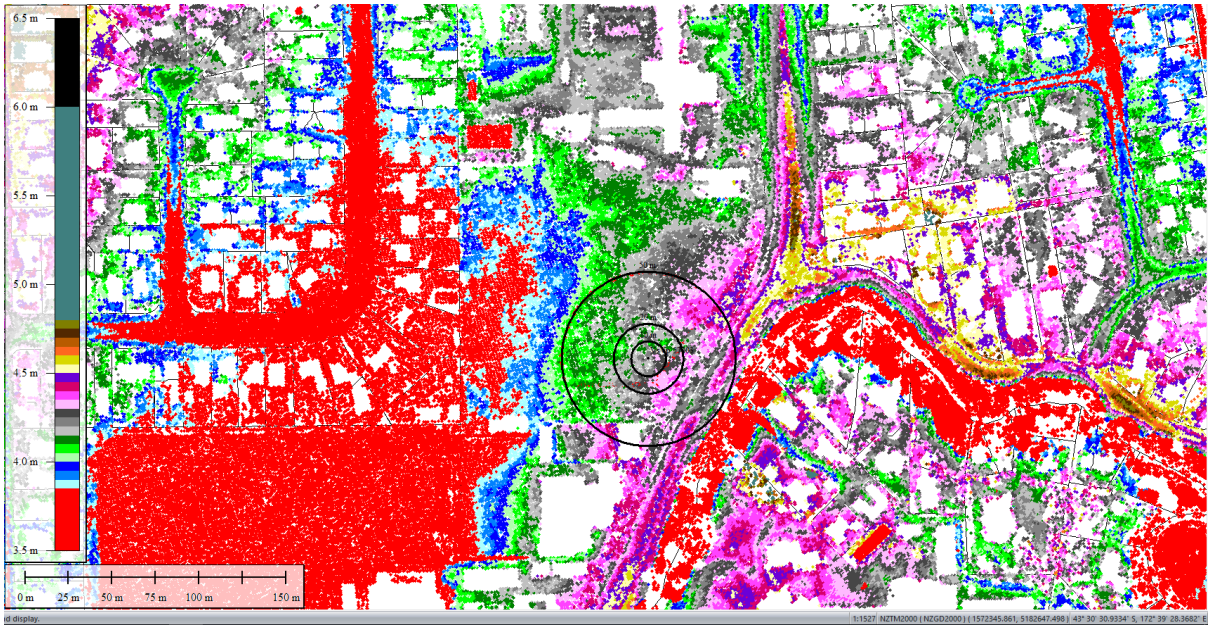

Figure 44: May 2011 LiDAR survey.

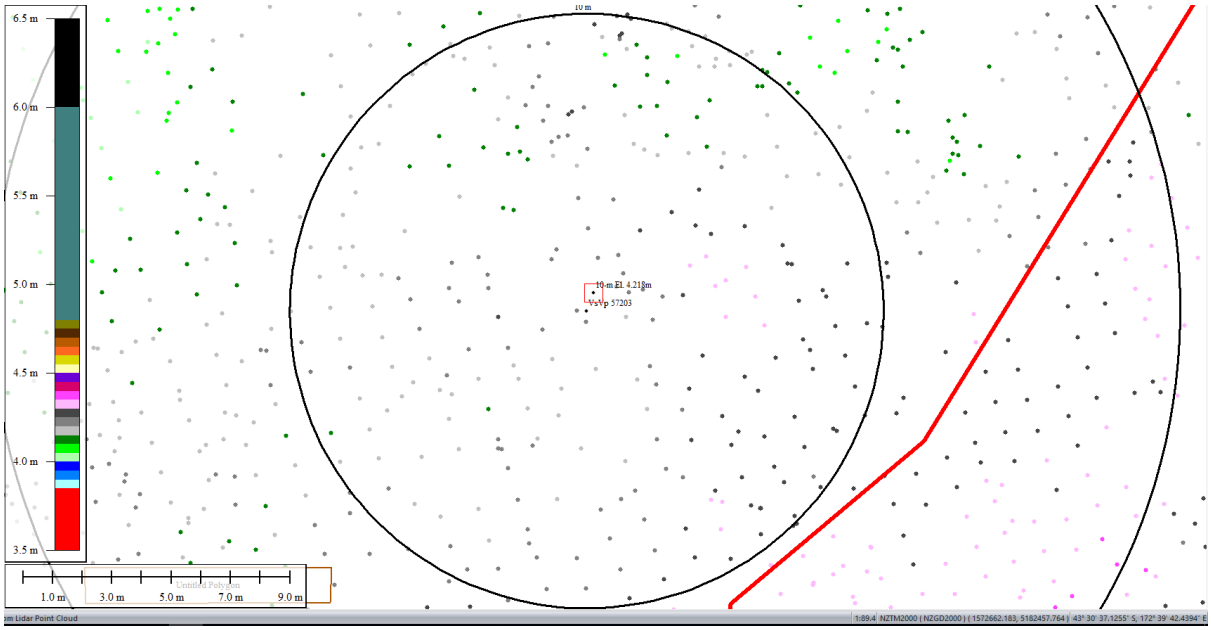

Figure 45: Ground surface elevation averaged over 10-m buffer for May 2011 LiDAR survey.

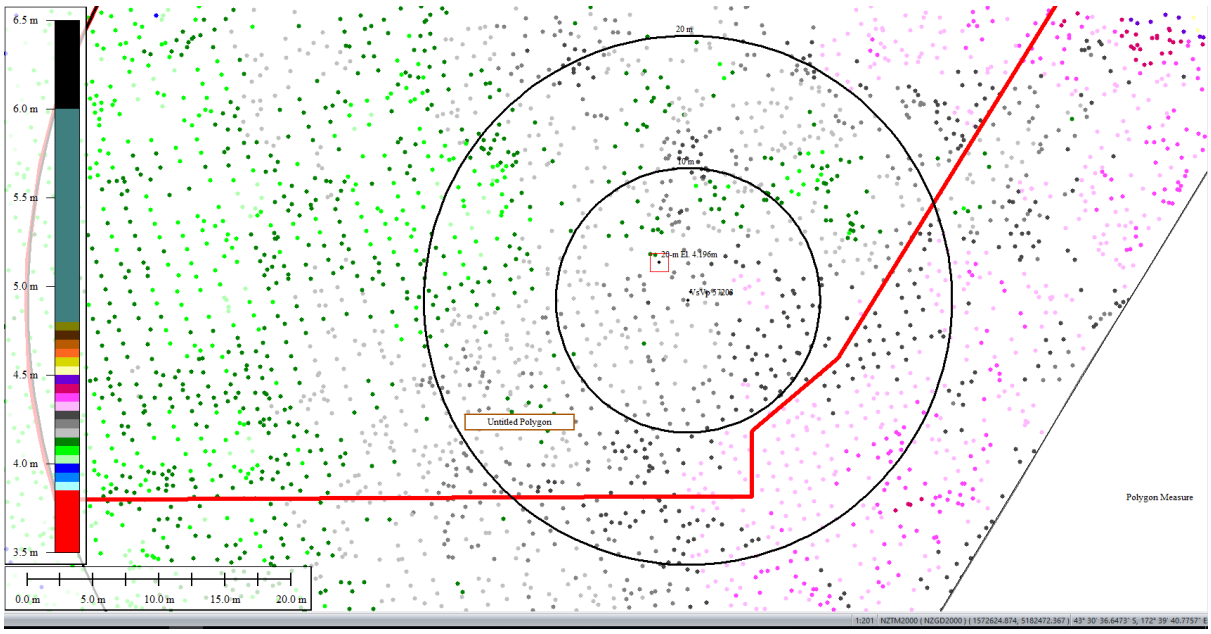

Figure 46: Ground surface elevation averaged over 20-m buffer for May 2011 LiDAR survey.

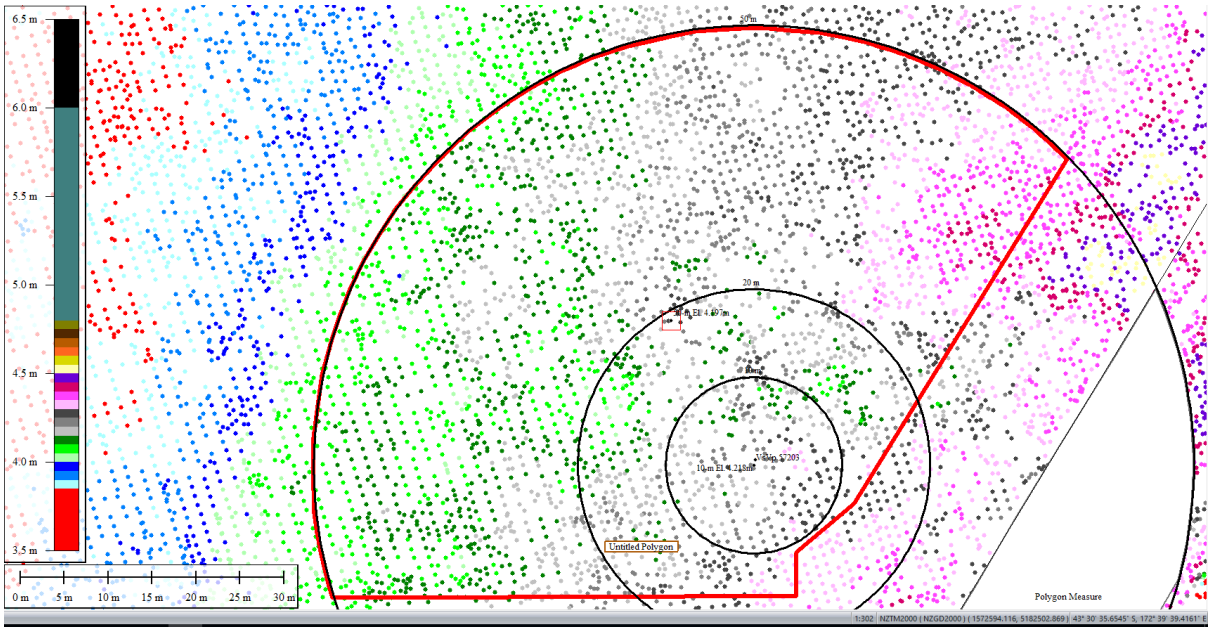

Figure 47: Ground surface elevation averaged over 50-m buffer for May 2011 LiDAR survey.

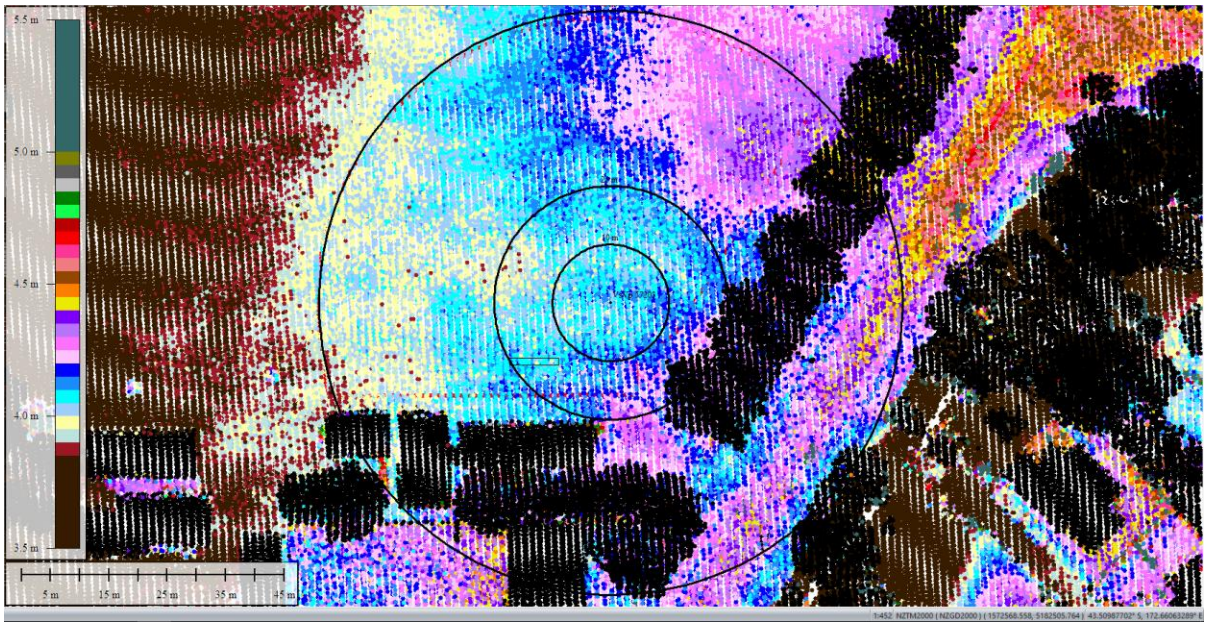

Figure 48: Sep 2011 LiDAR survey.

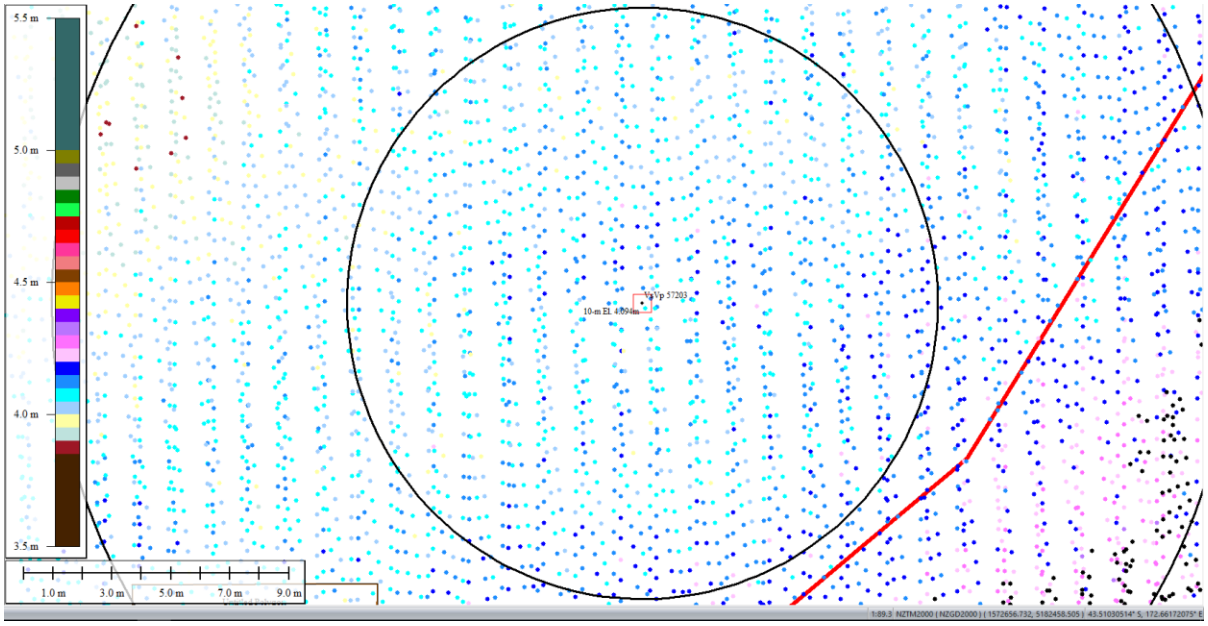

Figure 49: Ground surface elevation averaged over 10-m buffer for Sep 2011 LiDAR survey.

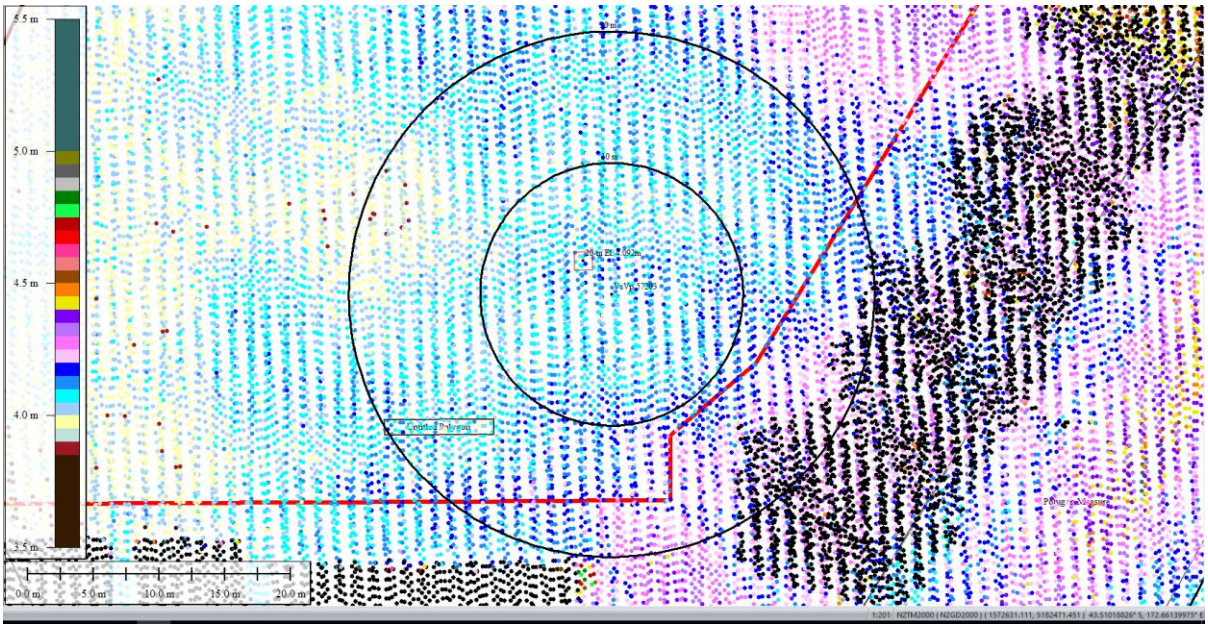

Figure 50: Ground surface elevation averaged over 20-m buffer for Sep 2011 LiDAR survey.

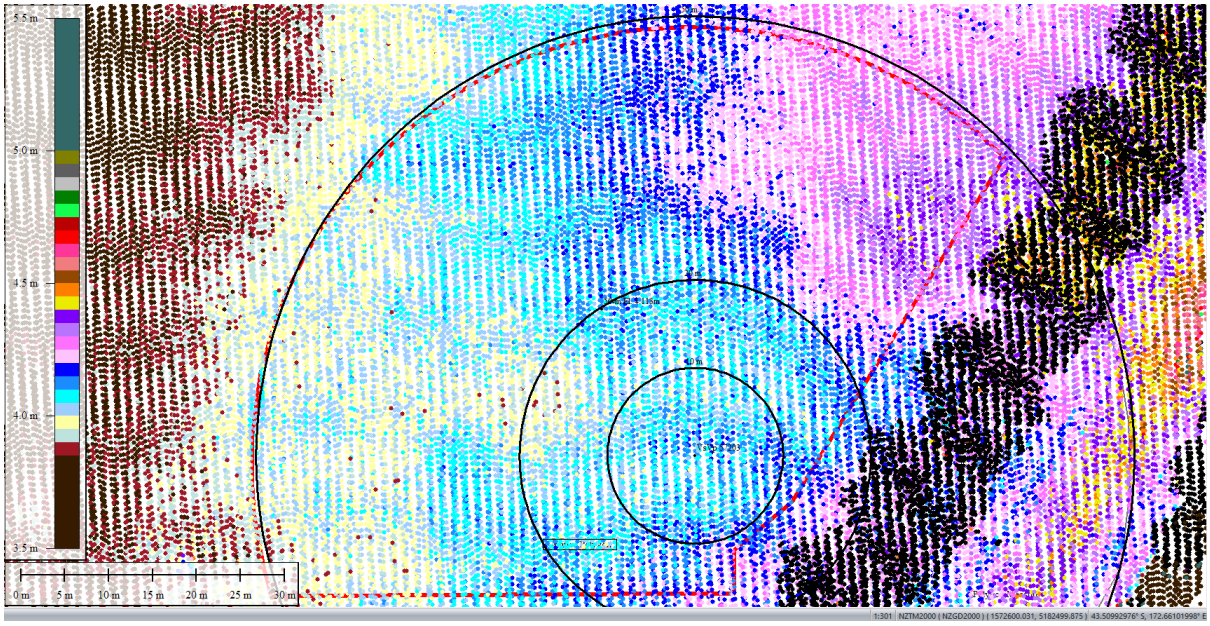

Figure 51: Ground surface elevation averaged over 50-m buffer for Sep 2011 LiDAR survey.

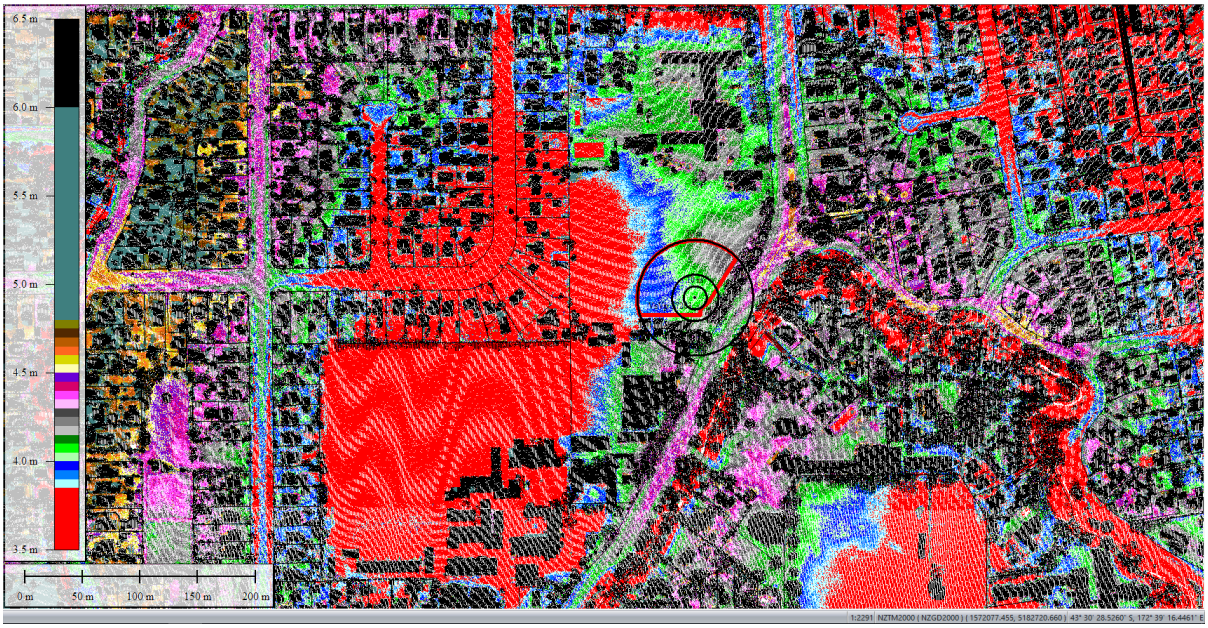

Figure 52: Feb 2012 LiDAR survey.

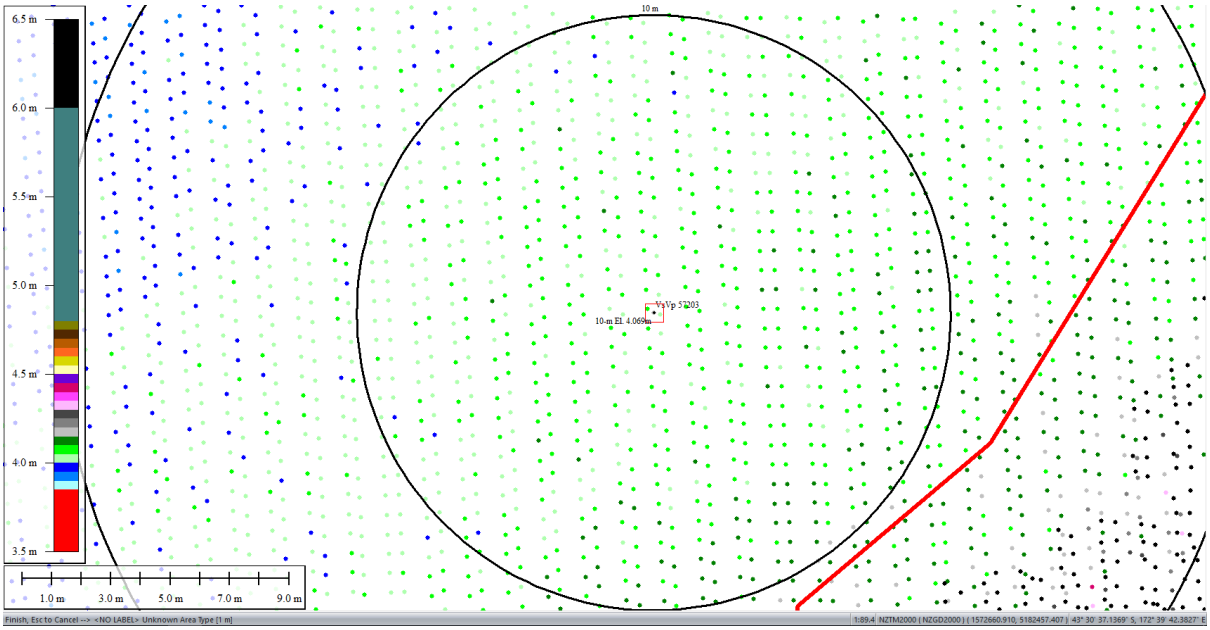

Figure 53: Ground surface elevation averaged over 10-m buffer for Feb 2012 LiDAR survey.

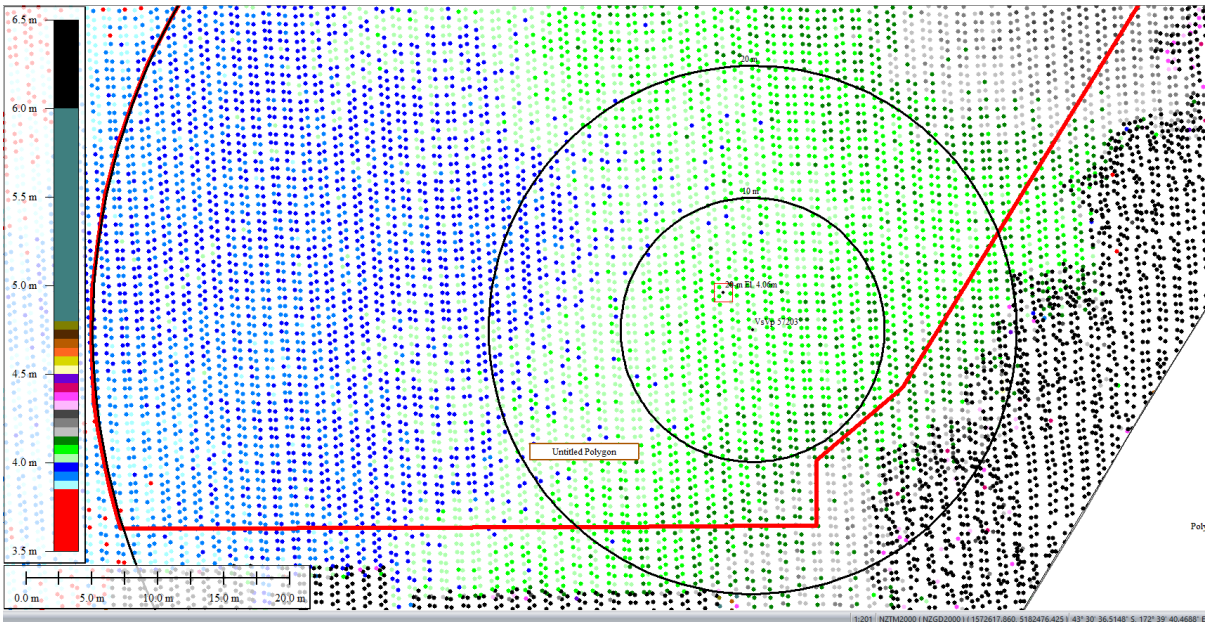

Figure 54: Ground surface elevation averaged over 20-m buffer for Feb 2012 LiDAR survey.

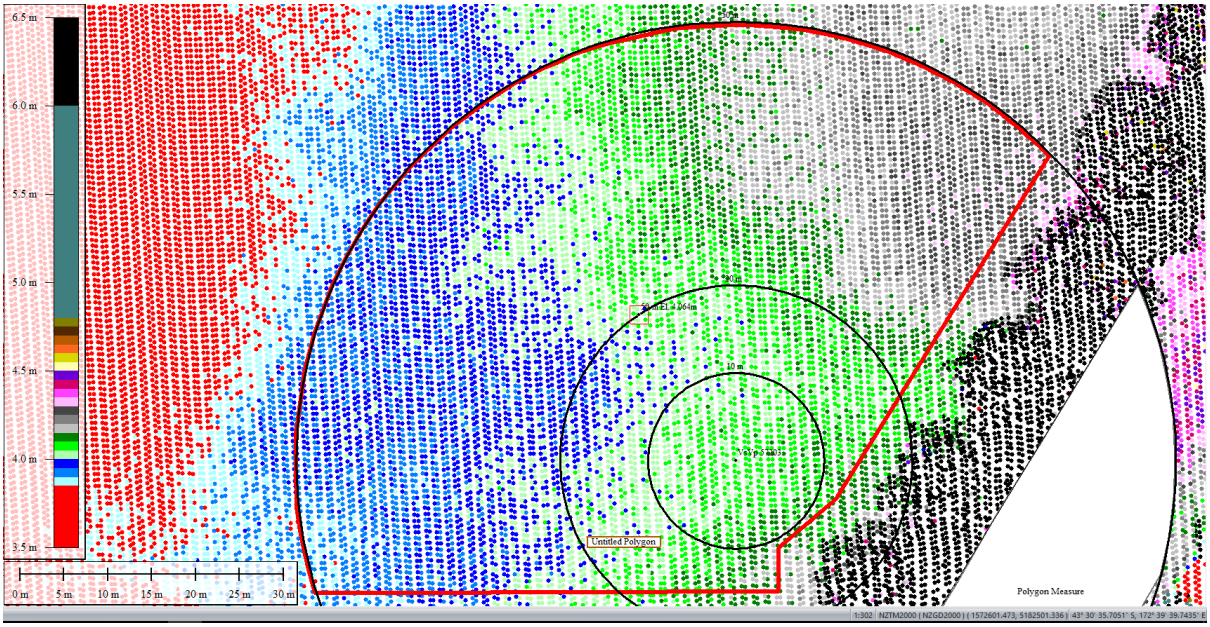

Figure 55: Ground surface elevation averaged over 50-m buffer for Feb 2012 LiDAR survey.

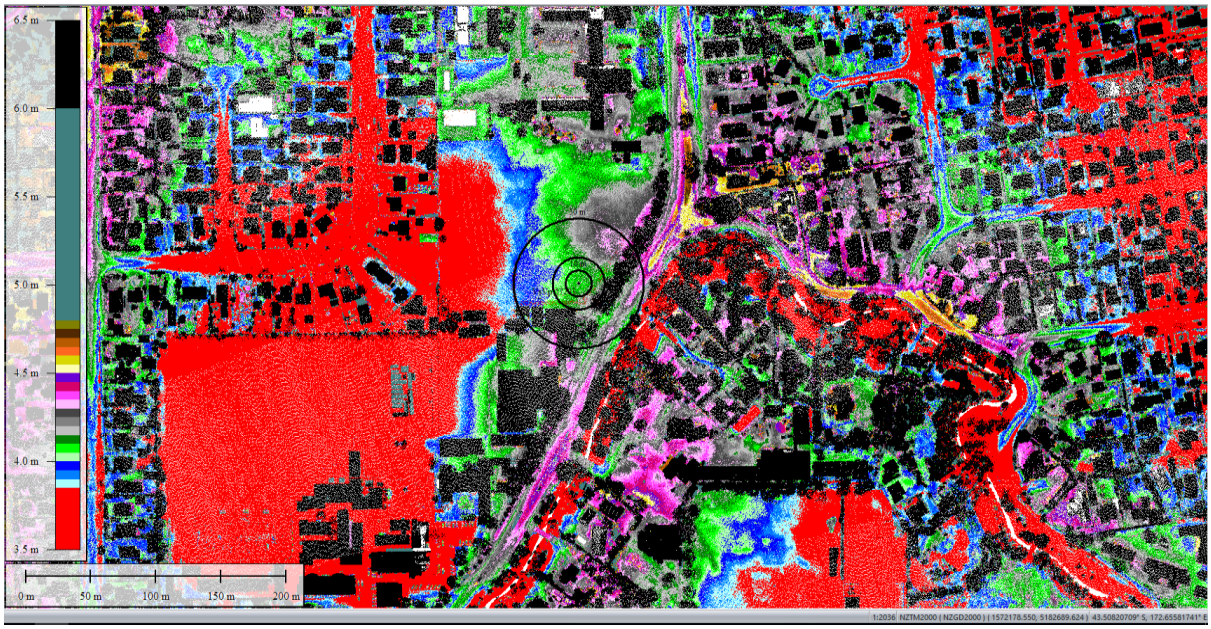

Figure 56: Oct 2015 LiDAR survey.

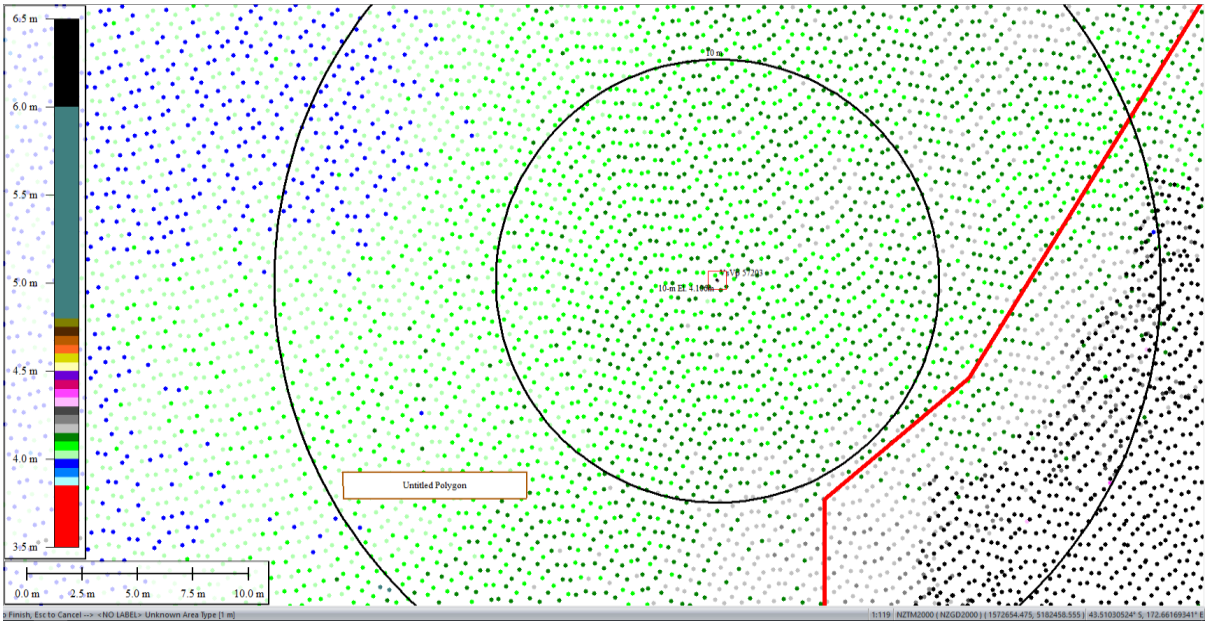

Figure 57: Ground surface elevation averaged over 10-m buffer for Oct 2015 LiDAR survey.

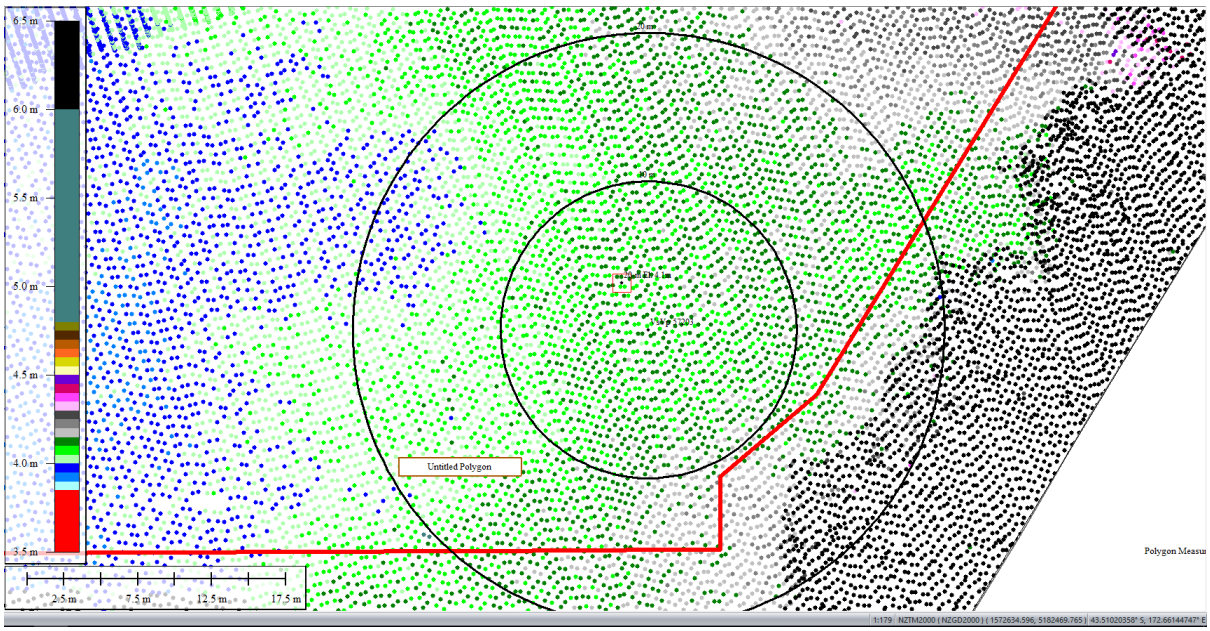

Figure 58: Ground surface elevation averaged over 20-m buffer for Oct 2015 LiDAR survey.

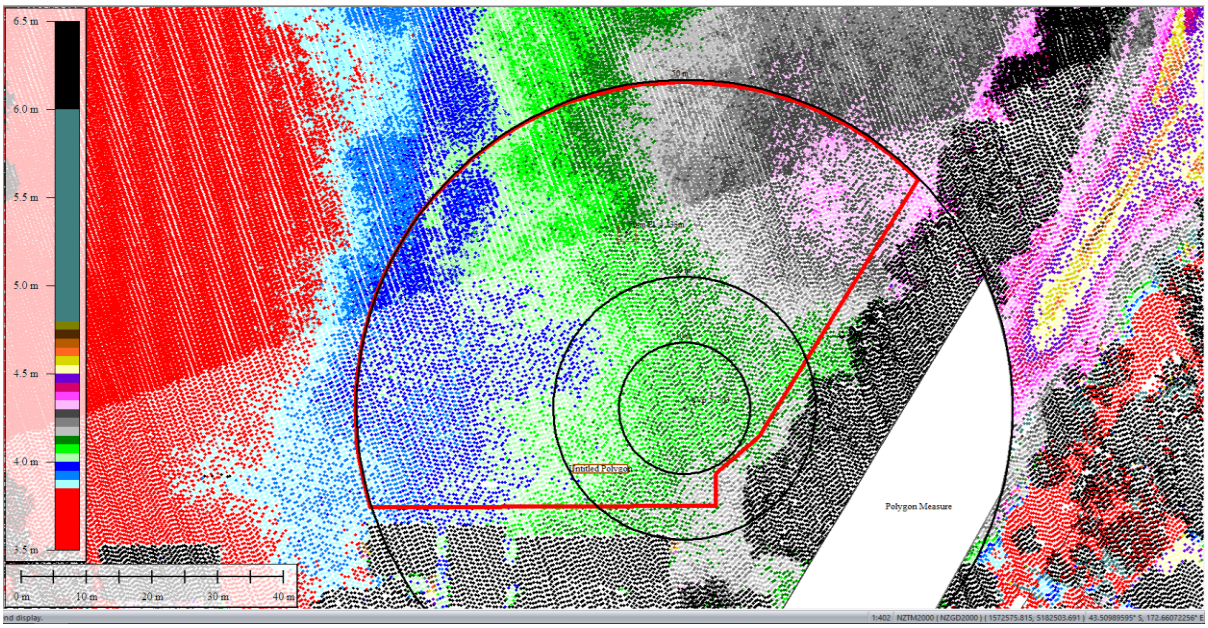

Figure 59: Ground surface elevation averaged over 50-m buffer for Oct 2015 LiDAR survey.

Figure 60: Ejecta outline for Sep-10 EQ.

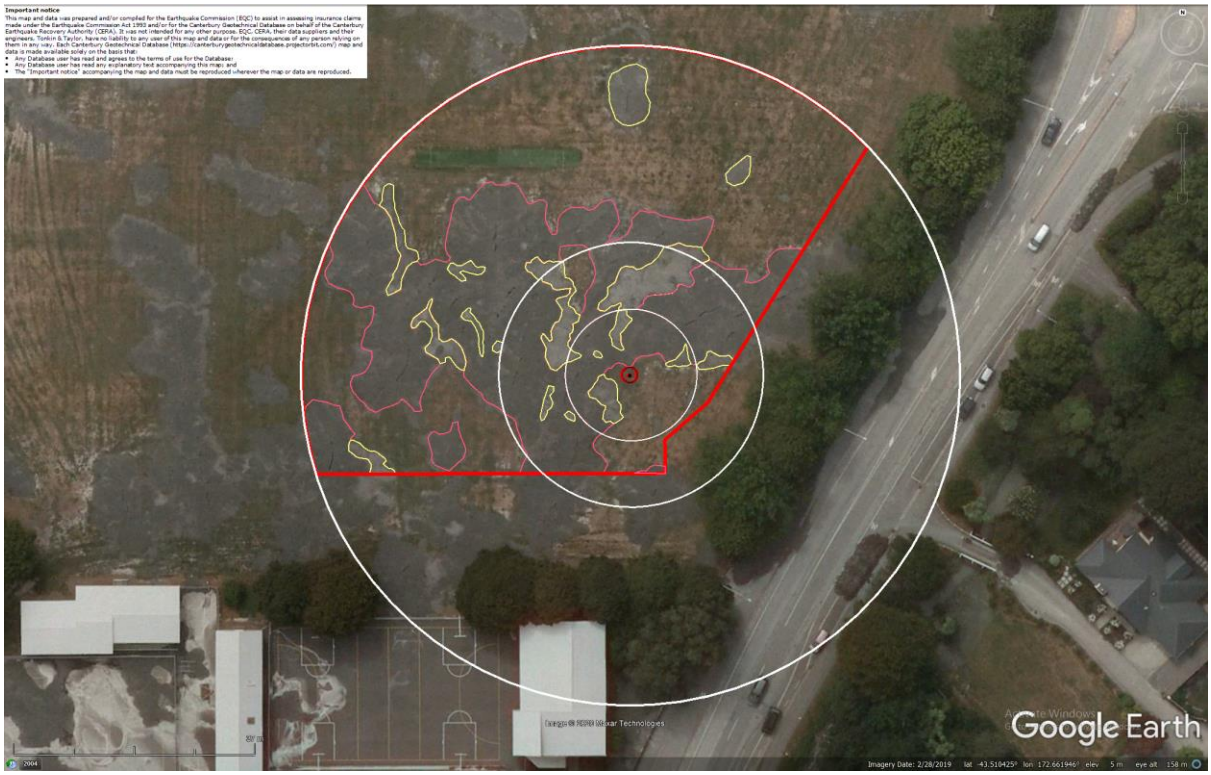

Figure 61: Ejecta outline for Feb-11 EQ.

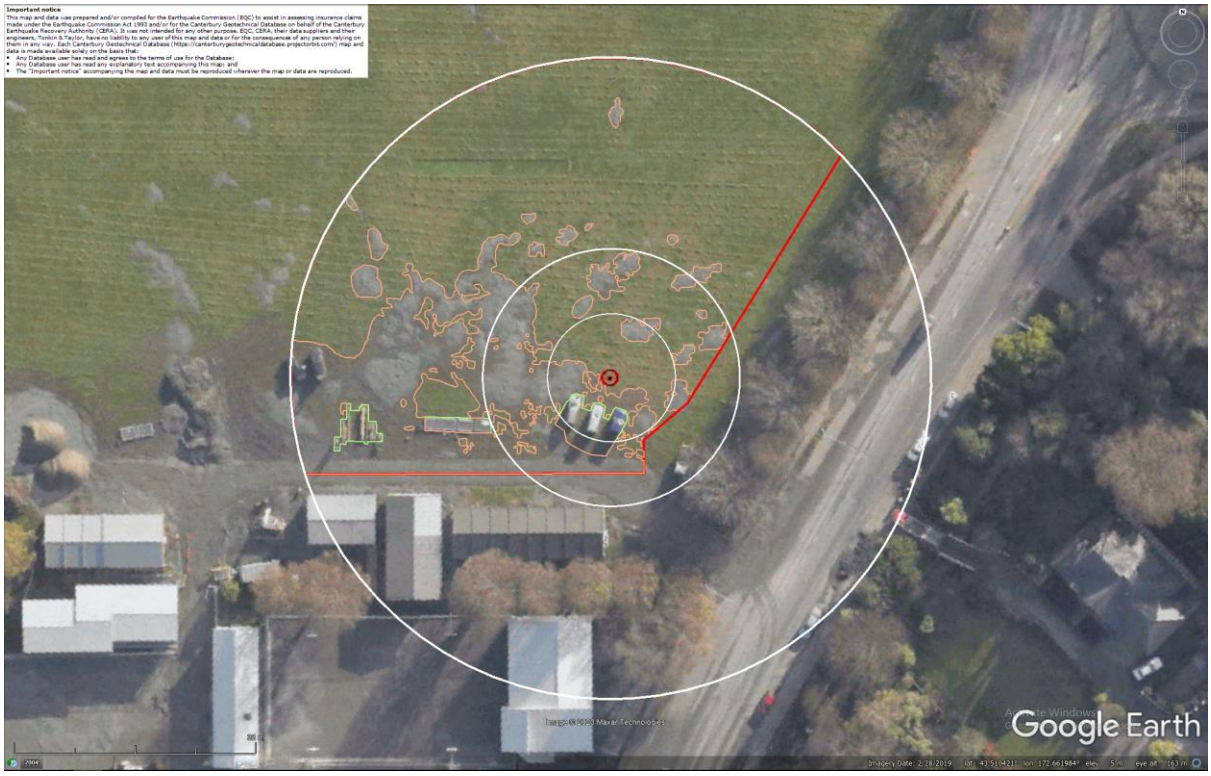

Figure 62: Ejecta outline for Jun-11 EQ.

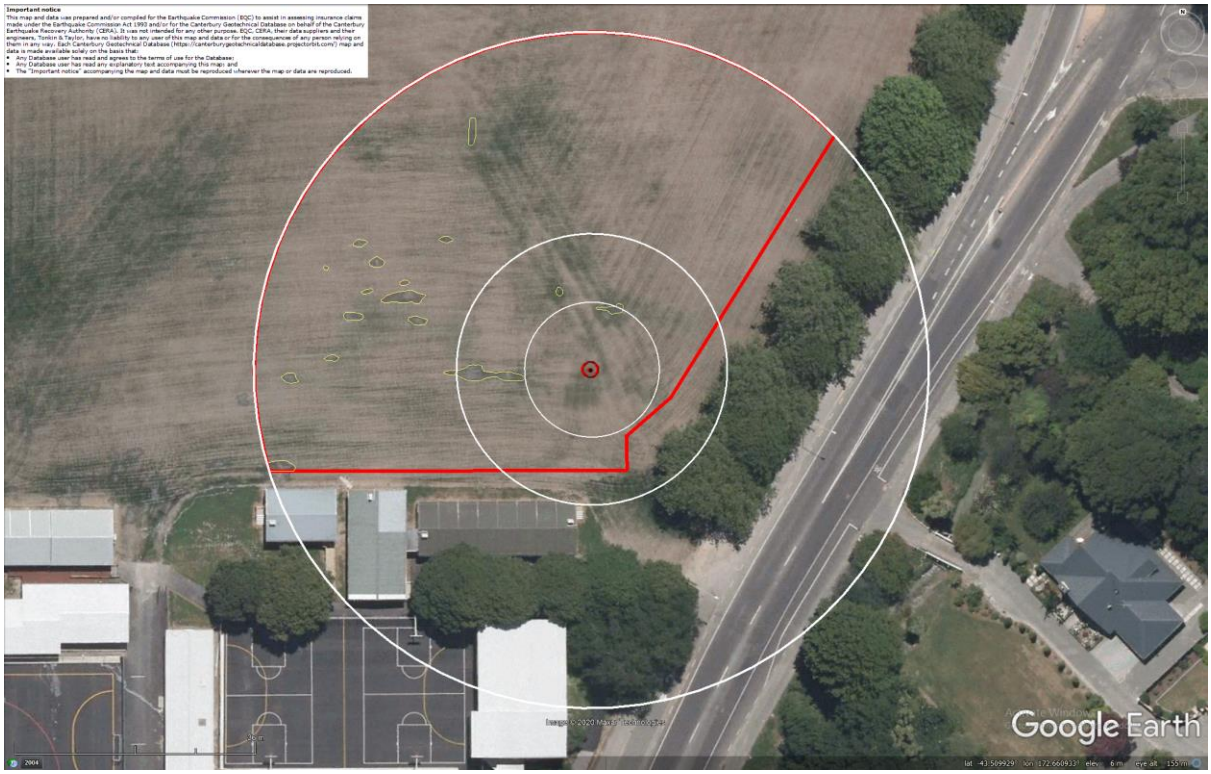

Figure 63: Ejecta outline for Dec-11 EQ.

Figure 64. Locations of Cone Penetration Tests (CPTs).

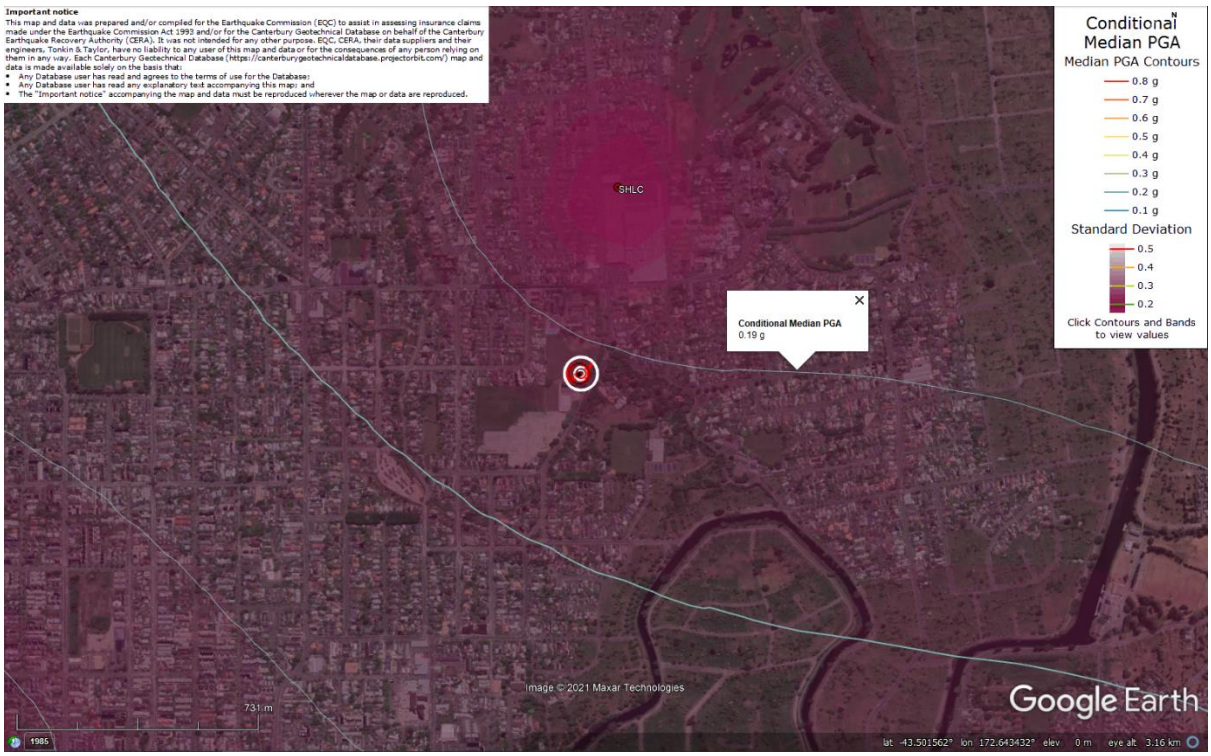

Figure 65. PGA for Sep-10 EQ (st. dev. = 0.250-0.275 ln units).

Figure 66. PGA for Feb-11 EQ (st. dev. = 0.275-0.300 ln units).

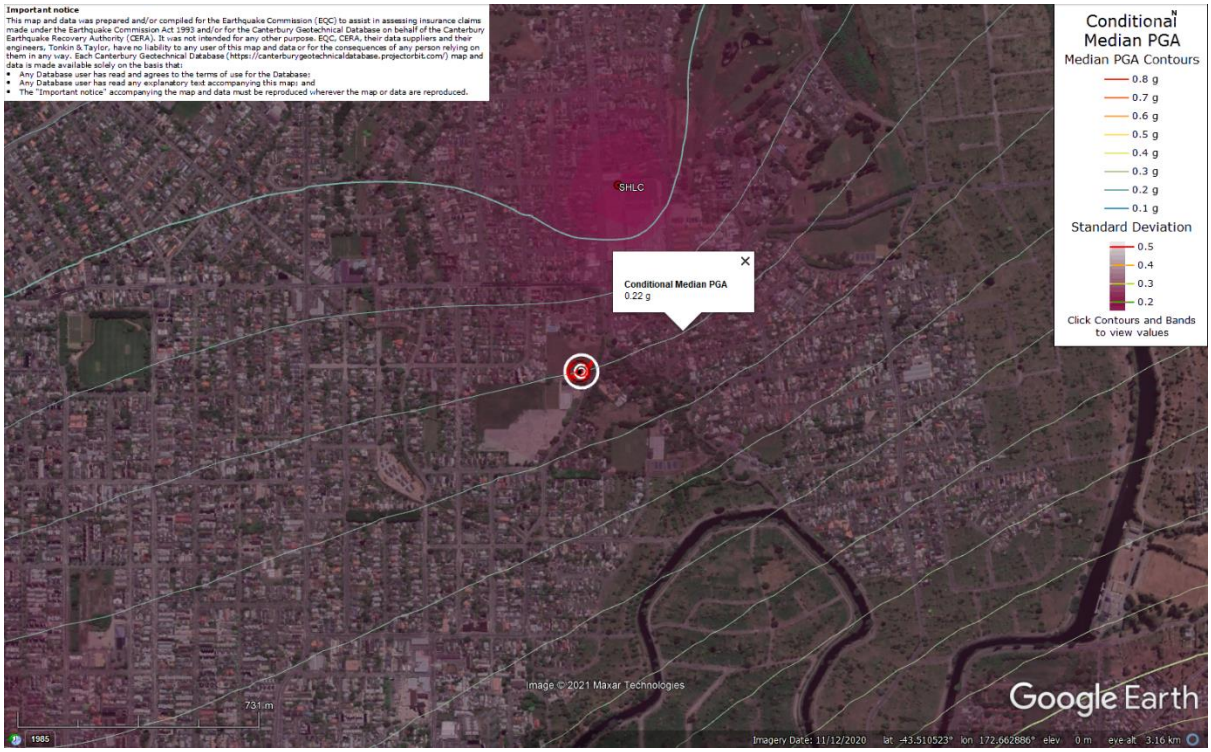

Figure 67. PGA for Jun-11 EQ (st. dev. = 0.275-0.300 ln units).

Figure 68. PGA for Dec-11 EQ (st. dev. = 0.300-0.325 ln units).

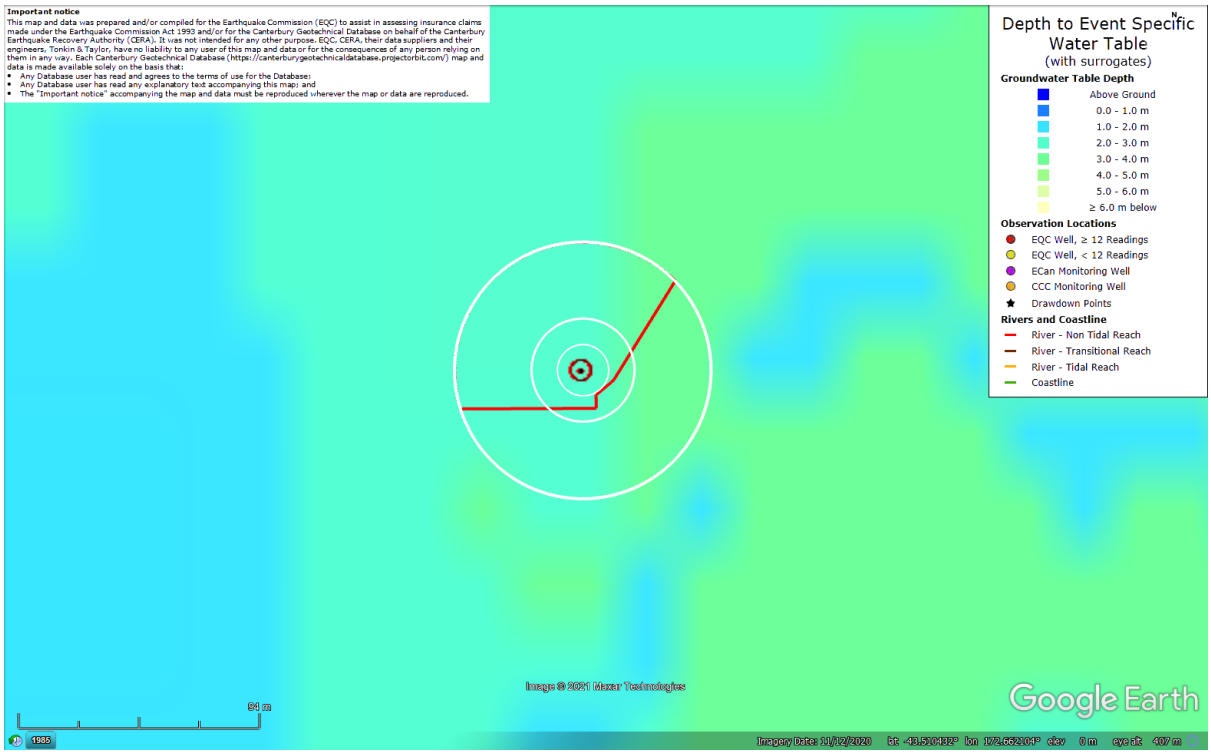

Figure 69. Depth to groundwater table for Sep-10 EQ.

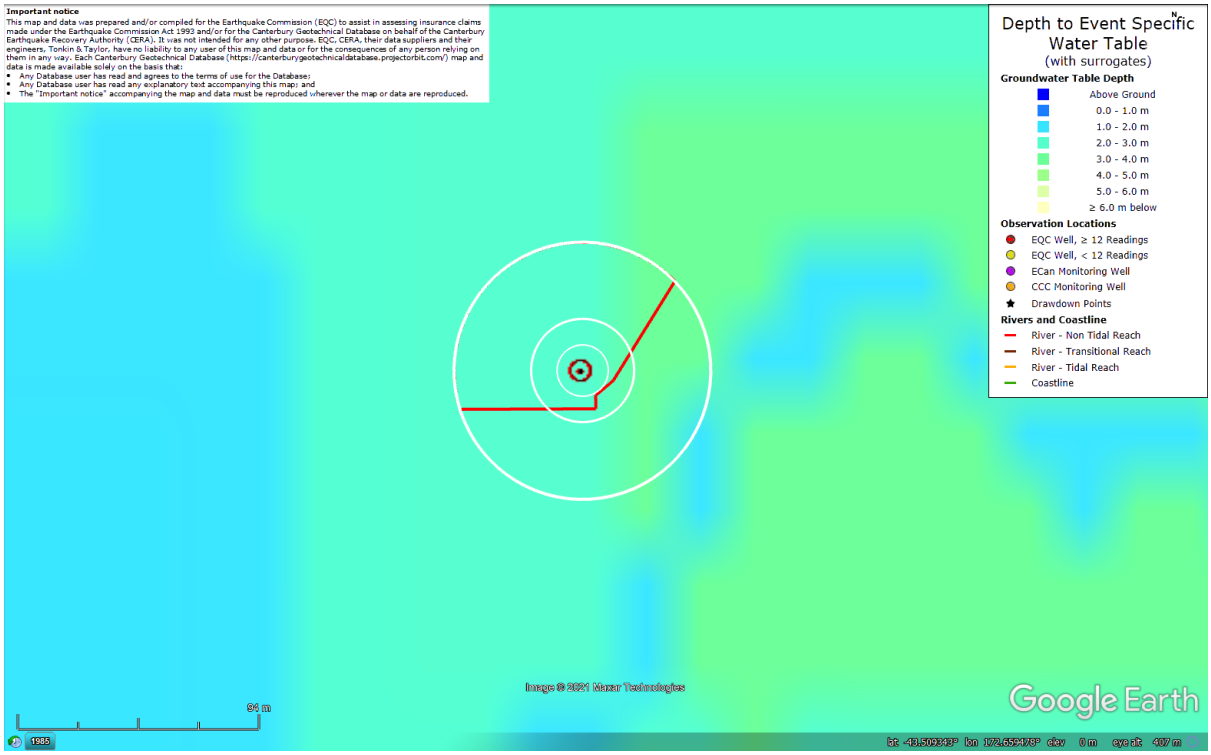

Figure 70. Depth to groundwater table for Feb-11 EQ.

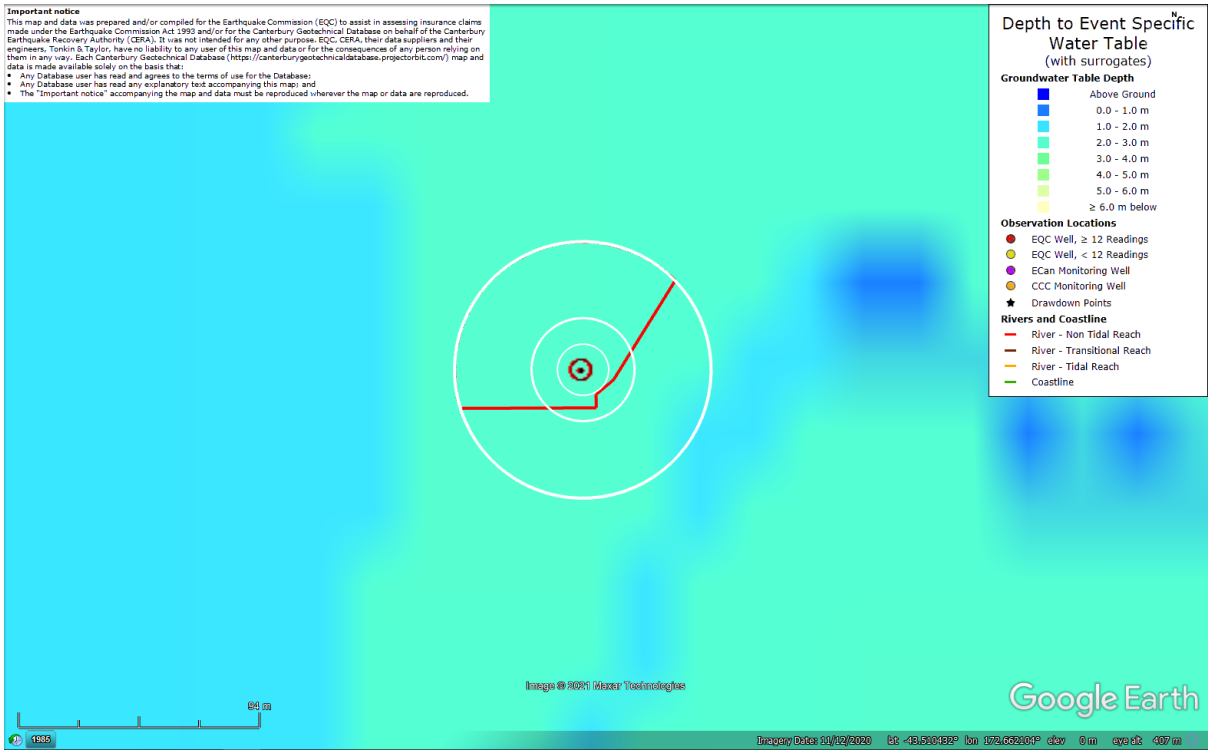

Figure 71. Depth to groundwater table for Jun-11 EQ.

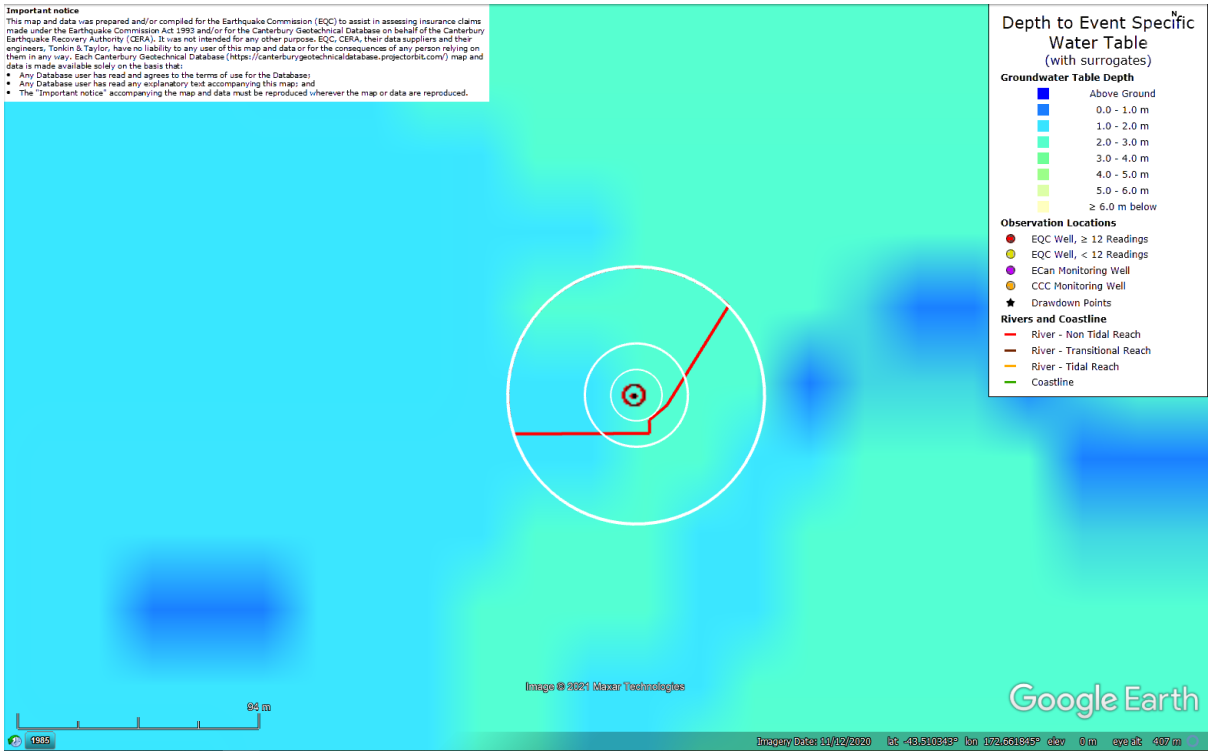

Figure 72. Depth to groundwater table for Dec-11 EQ.

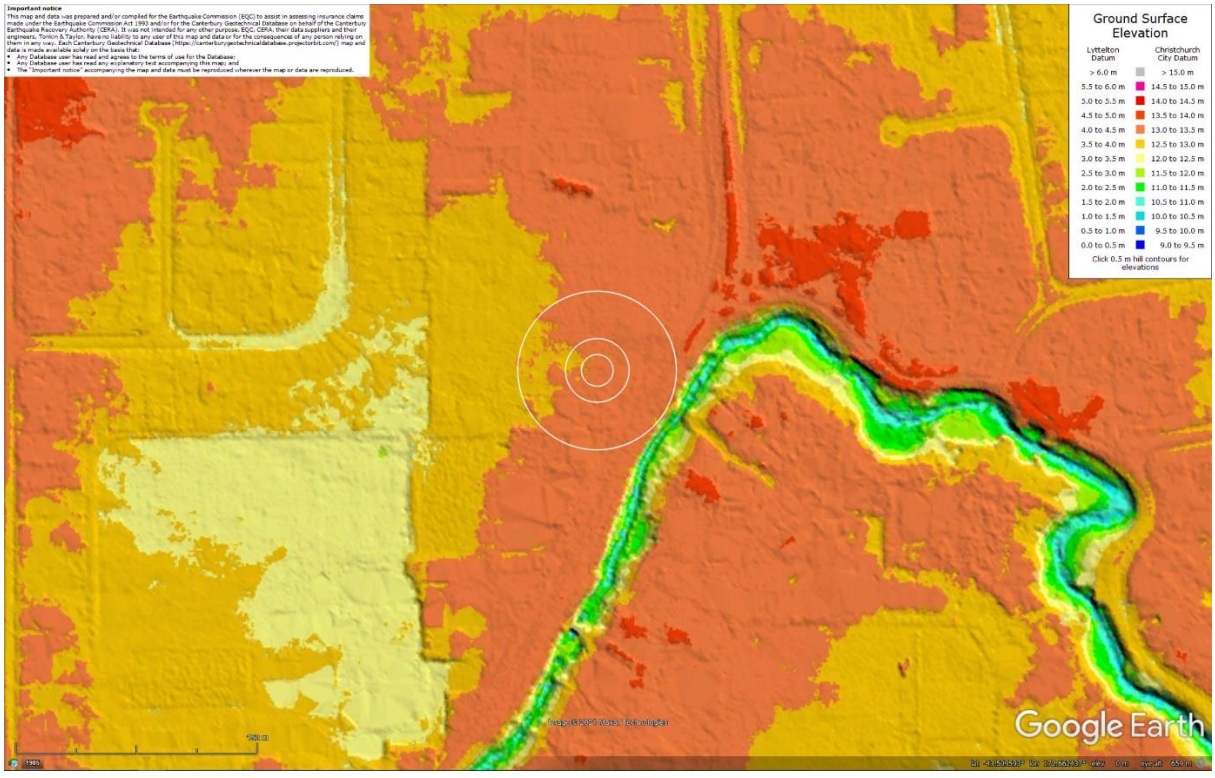

Figure 73. Ground surface elevation according to the Sep-11 LiDAR survey.

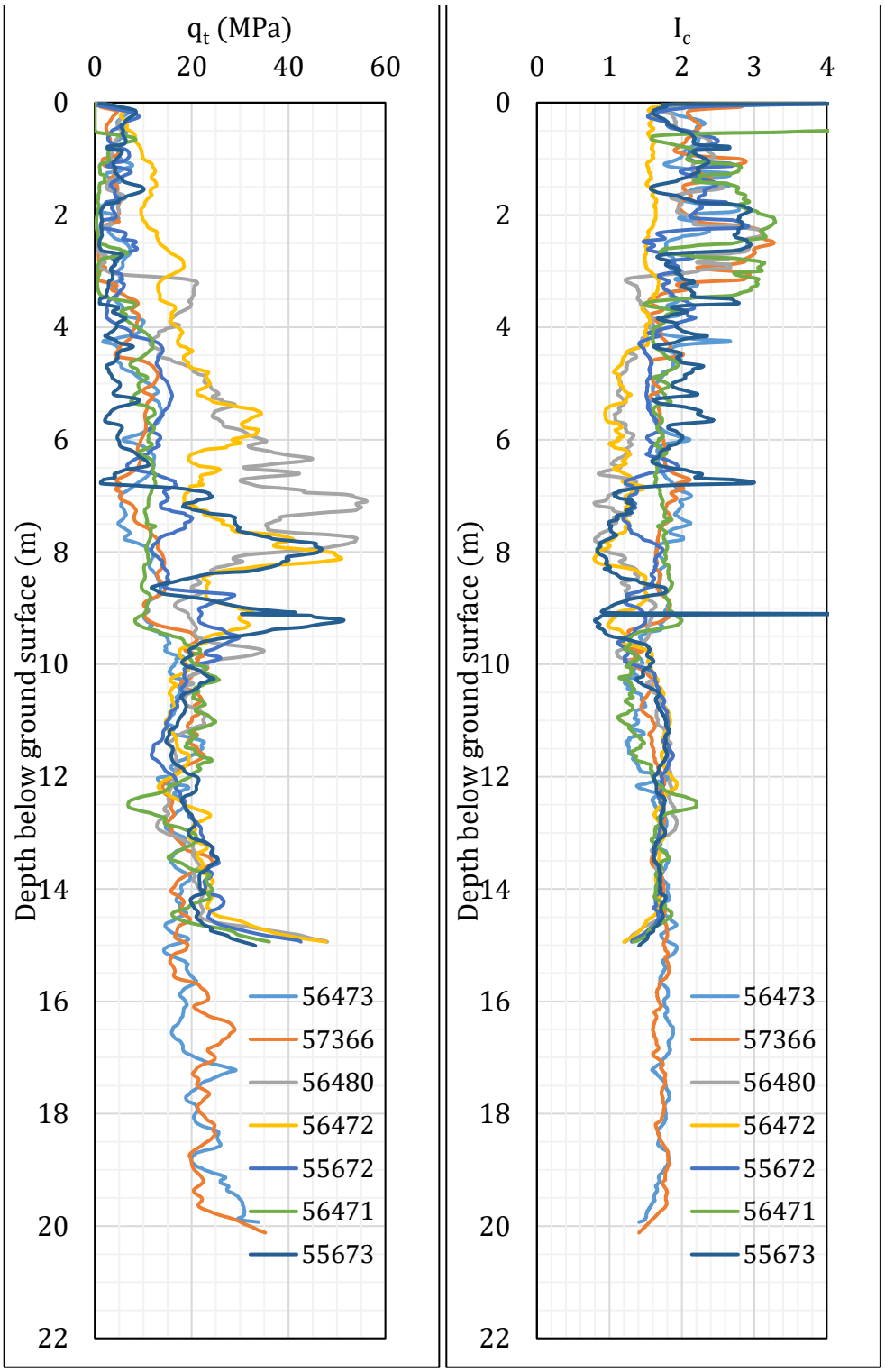

Figure 74. q_t and I_c profiles.

Note 6: The selection of CPTs for the area considered for settlement assessment (Figure 1) is based on the proximity of the CPTs to the considered areas. In accordance with that, the following table shows CPTs that were used for the volumetric settlement analysis in *Cliq v.3.0.3.2*, a CPT soil liquefaction software developed by GeoLogismiki. (The average volumetric settlements were reported in Table 8.)

Table 12: CPT profiles used in volumetric settlement analysis for areas selected for settlement assessment.

CPT ID No.	10 m-buffer	20-m buffer	50-m buffer
56473 (4065)	✓	✓	✓
57366 (56891)	✓	✓	✓
56480 (4079)			✓
56472 (4064)			✓
55672 (4066)			✓
55673 (4068)			
56471 (4063)			✓

Table 13: CPT-based results.

		CPT ID					
EQ Event	Parameter	56473	57366	56480	56472	55672	56471
Sep-10	S_{V1D} (mm)	7	7	1	0	4	1
	LSN	1	1	0	0	1	0
	LPI	0	0	0	0	0	0
	LPI_{ish}	0	0	0	0	0	0
	$D_{FS<1}$ (m)	undet.	undet.	undet.	undet.	undet.	undet.
Feb-11	S_{V1D} (mm)	71	70	7	0	43	36
	LSN	13	13	2	0	11	7
	LPI	5	5	1	0	4	1
	LPI_{ish}	3	4	1	0	3	1
	$D_{FS<1}$ (m)	3.20	3.18	undet.	undet.	2.72	3.45
Jun-11	S_{V1D} (mm)	9	10	1	0	7	1
	LSN	2	2	1	0	2	0
	LPI	0	0	0	0	0	0
	LPI_{ish}	0	0	0	0	0	0
	$D_{FS<1}$ (m)	undet.	undet.	undet.	undet.	undet.	undet.
Dec-11	S_{V1D} (mm)	22	28	4	0	20	6
	LSN	4	6	1	0	6	1
	LPI	0	1	0	0	1	0
	LPI_{ish}	0	1	0	0	1	0
	$D_{FS<1}$ (m)	4.27	4.32	undet.	undet.	3.45	undet.

Notes: $D_{FS<1}$ = Depth to the first liquefiable layer (FS_L<1) that is at least 200-mm thick, as determined by the Boulanger and Idriss (2016) liquefaction-triggering procedure (P_L=50%, C_{FC}=0.13, and $I_{c,cutoff}$ =2.6), and exported from *Cliq v.3.0.3.2*; undet. = the specified soil layer was not detected.

Note 7: Based on the borehole log (BH 57258, Figure 64), the soil profile consists of (1) topsoil to a depth of 0.4 m, (2) interchangeable layers of non-plastic to low plasticity silt and silty sand, ML, the Yaldhurst members of the Springston formation, to a depth of 3.35 m, (3) poorly graded sand, SP, of

the Christchurch formation to a depth of 8.2 m, (4) sandy subrounded gravel, GW, of the Christchurch formation to a depth of 11.05 m, and (5) poorly graded sand, SP, of the Christchurch formation to a depth of 15.65 m (the end of the borehole). The nearby borehole (BH 62338, Figure 64) suggests that the SP-SW layer of the Christchurch formation extends to a depth of approximately 20 m, after which an ML layer of the Christchurch formation extends to a depth of roughly 25 m. The groundwater table is at an average depth of 2.3 m below the ground surface (the instrument, with readings from Aug 2012 to Feb 2017, is ~165 m to the NW at a ground surface elevation that is ~0.75 lower than the elevation of the site, which was accounted for in the 2.3-m depth). The laboratory test results are not available.

Note 8: The ejecta-induced free-field settlement provided in Table 11 is an areal average settlement due to ejecta, which is based on the total settlement assessment area, A_T (provided in Table 9 and repeated in Table 14). However, the considered area was not always covered completely with ejecta; thus, it is important to provide the localized ejecta-induced settlement, too. The localized settlement due to ejecta is estimated using photographic evidence only as

$$S_{E,P\_localized} = \frac{V_E}{A_E}$$

where V_E is the total volume of ejecta within A_T and A_E is the total coverage area of ejecta within A_T. Please note that the areal ejecta-induced settlement provided in Table 14 as S_{E,P_areal} is the same as $S_{E,P}$ in Table 11, which was estimated as

$$S_{E,P\_areal} = S_{E,P} = \frac{V_E}{A_T}$$

where V_E is the total volume of ejecta within A_T and A_T is the total settlement assessment area.

Table 14a: Areal and localized ejecta-induced settlement estimates for Patch A (10-m buffer) based on photographic evidence.

Earthquake Event	A_T (m^2)	A_E (m^2)	V_E (m^3)	S_{E,P_areal} (mm)	$S_{E,P\_localized}$ (mm)
Sep-10	314	0	0	0	0
Feb-11	314	182	23.4-39.7	100±25	175±45
Jun-11	269	94.0	2.8-9.4	25±10	65±35
Dec-11	314	3.0	0.03-0.06	<5	15±5

Notes: $S_{E,P\_areal} = S_{E,P}$ reported in Table 11 = areal ejecta-induced settlement; $S_{E,P\_localized}$ = localized ejecta-induced settlement; A_T = total settlement assessment area; V_E = total volume of ejecta within A_T; A_E = total area of ejecta within A_T; The estimates of both areal and localized ejecta-induced settlement are rounded to the nearest 5 mm; Final plus/minus values are also rounded to the nearest 5 mm.

Table 14b: Areal and localized ejecta-induced settlement estimates for Patch A (20-m buffer) based on photographic evidence.

Earthquake Event	A_T (m^2)	A_E (m^2)	V_E (m^3)	S_{E,P_areal} (mm)	$S_{E,P\_localized}$ (mm)
Sep-10	1003	0	0	0	0
Feb-11	1003	765	97.7-166	130±35	175±45
Jun-11	938	439	13.2-43.9	30±15	65±35
Dec-11	1003	18.0	0.18-0.36	<5	15±5

Notes: S_{E,P_areal} = $S_{E,P}$ reported in Table 11 = areal ejecta-induced settlement; $S_{E,P\_localized}$ = localized ejecta-induced settlement; A_T = total settlement assessment area; V_E = total volume of ejecta within A_T; A_E = total area of ejecta within A_T; The estimates of both areal and localized ejecta-induced settlement are rounded to the nearest 5 mm; Final plus/minus values are also rounded to the nearest 5 mm.

Table 14c: Areal and localized ejecta-induced settlement estimates for Patch A (50-m buffer) based on photographic evidence.

Earthquake Event	A_T (m^2)	A_E (m^2)	V_E (m^3)	S_{E,P_areal} (mm)	$S_{E,P\_localized}$ (mm)
Sep-10	4061	0	0	0	0
Feb-11	4061	1735	228-386	75±20	175±45
Jun-11	3944	1191	35.7-119	20±10	65±35
Dec-11	4061	55.0	0.6-1.1	<5	15±5

Notes: S_{E,P_areal} = $S_{E,P}$ reported in Table 11 = areal ejecta-induced settlement; $S_{E,P\_localized}$ = localized ejecta-induced settlement; A_T = total settlement assessment area; V_E = total volume of ejecta within A_T; A_E = total area of ejecta within A_T; The estimates of both areal and localized ejecta-induced settlement are rounded to the nearest 5 mm; Final plus/minus values are also rounded to the nearest 5 mm.

Summary 2:

The best estimate of the localized ejecta-induced free-field ground settlement at the Shirley Intermediate School site for the SEP 2010, FEB 2011, JUN 2011, and DEC 2011 earthquake is 0 mm, 175±45 mm, 65±35 mm, and 15±5 mm, respectively.

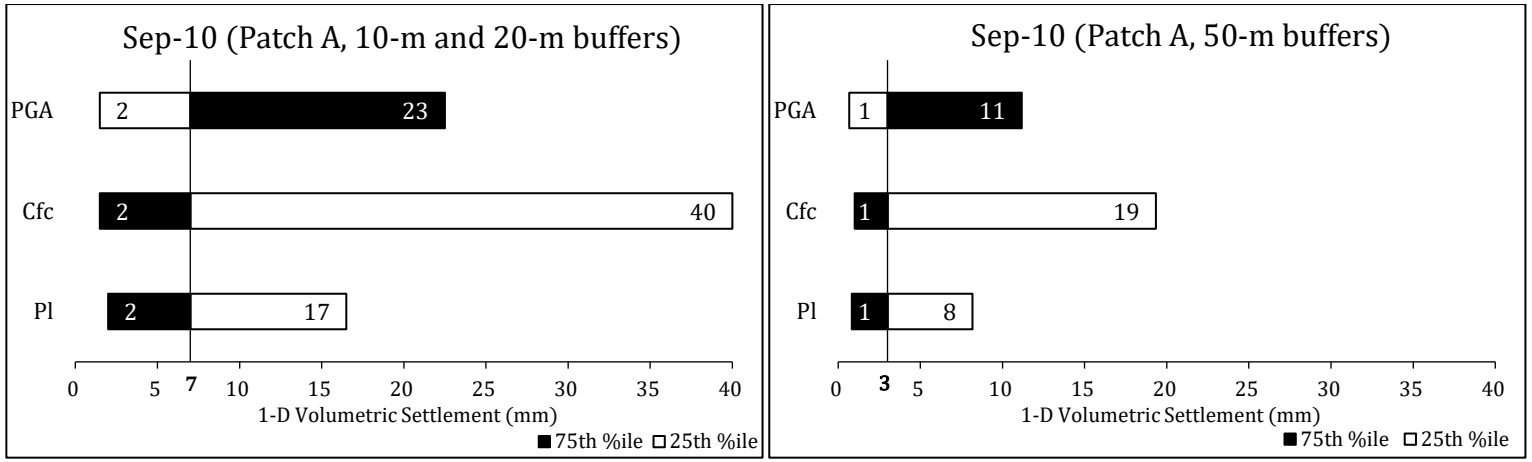

Figure 75: Sensitivity of volumetric settlement (Zhang et al. 2002) to PGA, C_{FC}, and P_L for Sep-10 EQ. (The baseline case is the 50th %ile.)

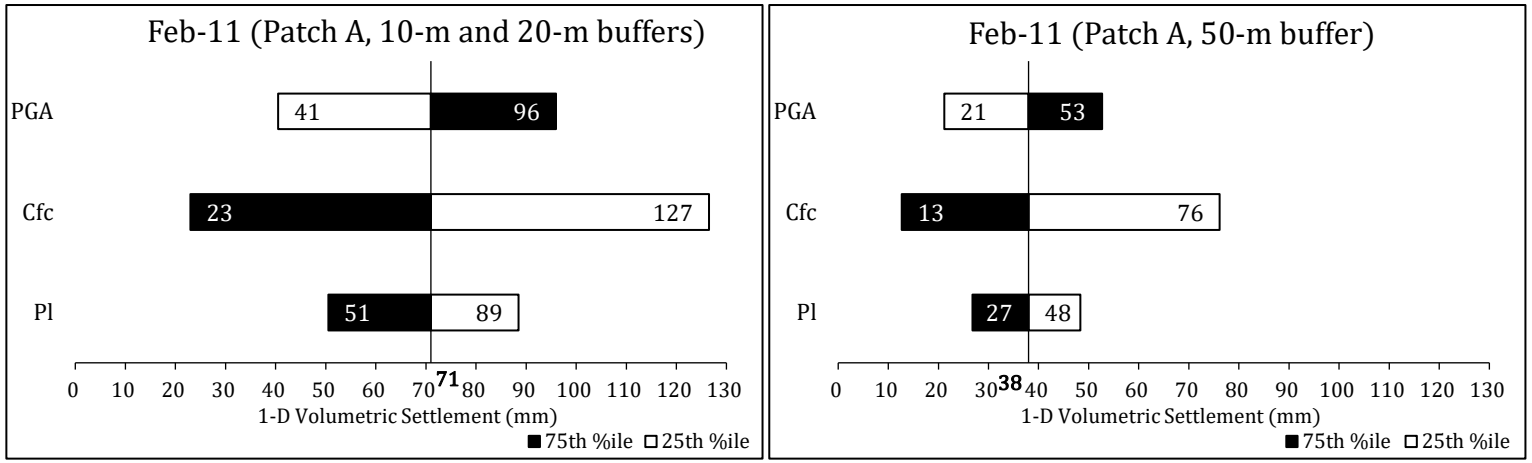

Figure 76: Sensitivity of volumetric settlement (Zhang et al. 2002) to PGA, C_{FC}, and P_L for Feb-11 EQ. (The baseline case is the 50th %ile.)

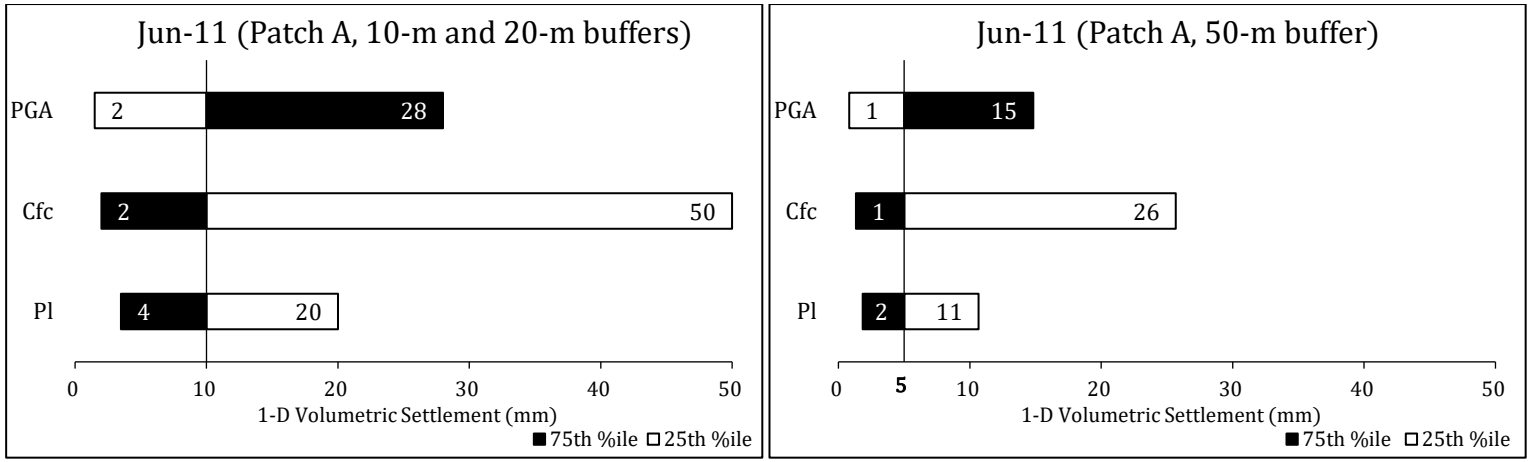

Figure 77: Sensitivity of volumetric settlement (Zhang et al. 2002) to PGA, C_{FC}, and P_L for Jun-11 EQ. (The baseline case is the 50th %ile.)

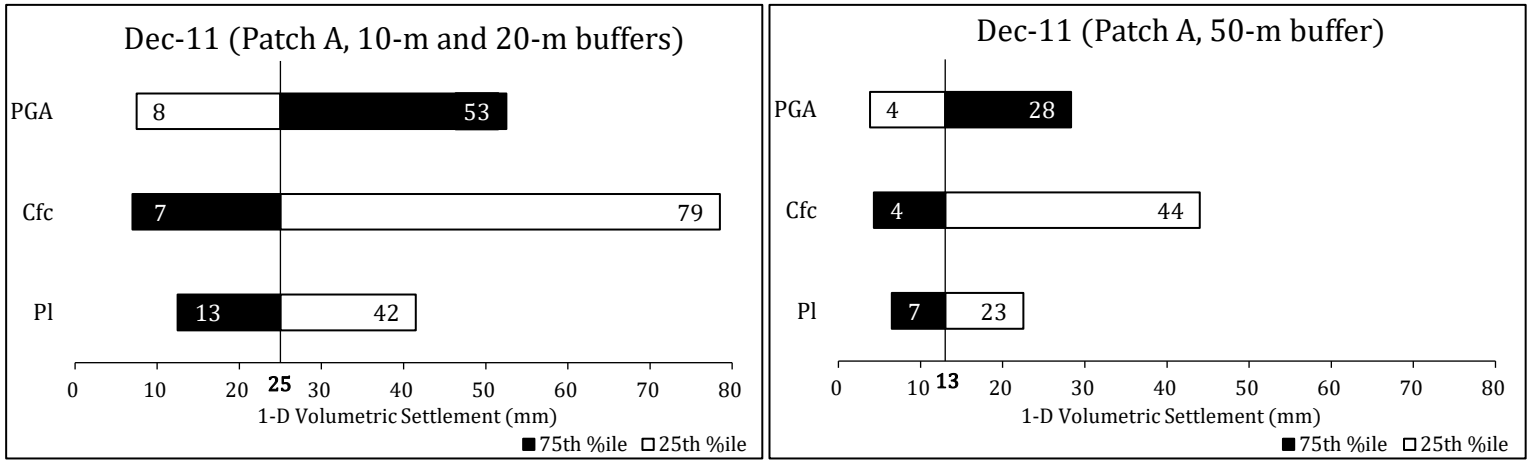

Figure 78: Sensitivity of volumetric settlement (Zhang et al. 2002) to PGA, C_{FC}, and P_L for Dec-11 EQ. (The baseline case is the 50th %ile.)